P516763.PDF [Page: 3 of 57]

Copy No. 8

DEFENCE R&D DÉFENSE

ADAPTIVE ARRAY PROCESSING IN A WIDEBAND REVERBERANT ENVIRONMENT

Dr. D. N. Swingler
Division of Engineering
Saint Mary's University
Halifax, N.S., Canada B3H 3C3

Defence R&D Canada

DEFENCE RESEARCH ESTABLISHMENT ATLANTIC

Contractor Report

DREA CR 2001-120

October 2001

National Defence Défense nationale

Canada

P516763.PDF [Page: 4 of 57]

104-07013/

Copy No: _____

Adaptive Array Processing in a Wideband Reverberant Environment

Dr David N. Swingler
Division of Engineering
Saint Mary's University
Halifax, NS, Canada B3H 3C3

Contract Number
W7707-5-3340/001/HAL

Defence Research Establishment Atlantic

Contractor Report

DREA CR 2001-120

October 2001

P516763.PDF [Page: 5 of 57]

Author

Dr. David N. Swingler

Approved by

Dr. Joseph N. Maksym

Scientific Authority

Approved for release by

Kirk Foster

Chair / Document Review Panel

The scientific or technical validity of this Contract Report is entirely the responsibility of the contractor and the contents do not necessarily have the approval or endorsement of Defence R&D Canada

© Her Majesty the Queen as represented by the Minister of National Defence, 2001

© Sa majesté la reine, représentée par le ministre de la Défense nationale, 2001

P516763.PDF [Page: 6 of 57]

Abstract

This contractor's report contains a detailed account of numerical simulations designed to measure the performance of various beamforming methods in highly-reverberant wideband environments. The Minimum-Variance Distortionless-Response (MVDR) method is used in conjunction with a horizontal array of limacon sensors and a horizontal parallel array of omnidirectional sensors. The benefits and drawbacks of both configurations are weighed and discussed. Additionally, mathematical models for all scenarios discussed in this report are examined.

Résumé

Le rapport de cet entrepreneur rend compte de façon détaillée de simulations numériques destinées à mesurer la performance de diverses méthodes de conformation de faisceaux dans des environnements à large bande présentant une forte réverbération. La méthode MVDR (Minimum-Variance Distortionless-Response) est utilisée conjointement avec un réseau horizontal de capteurs de type limaçon et un réseau parallèle horizontal de capteurs omnidirectionnels. Les avantages et les inconvénients de ces deux configurations sont évalués et discutés. En outre, des modèles mathématiques de tous les scénarios étudiés dans le rapport sont examinés.

P516763.PDF [Page 7 of 57]

This page intentionally left blank.

P516763.PDF [Page: 5 of 57]

Executive summary

Introduction

Reverberation caused by the reflection of active sonar pulses from surface waves, undersea topography or inhomogeneities in the water column usually forms the background against which target echoes must be detected. The signals from a towed line array of sensors are beamformed in order to attenuate background noise and reverberation, and to determine the direction of the target of interest. Low-frequency active sonar (LFA) generally operates in a frequency range where it becomes feasible to include horizontal dipole sensors in the towed array. The signals from these sensors can be combined with the omnidirectional signals to form limaçon directional sensitivity patterns in the horizontal plane. These limaçons can be steered to the left or right to resolve the directional ambiguity inherent in straight-line arrays of omindirectional sensors. In the same way, they can be used to attenuate interfering noise or reverberation arriving from the side of the array opposite to the target. An alternative method to provide left/right discrimination involves towing two parallel, closely-spaced arrays .

Under many conditions an improvement in the discrimination against background interference may be achieved by using adaptive beamforming, in which the beamformer weights are varied to optimize specified performance criteria. However, the evolution with time of the reverberation, and the existence of multipath propagation to the receive array present challenges that tend to degrade the performance of most adaptive beamformers. This study uses simulations to compare the performance of conventional and adaptive beamformers and the types of line array mentioned above under conditions typical of an LFA sonar.

Results

Attention is focussed in this report on the Minimum-Variance Distortionless Response (MVDR) adaptive beamformer. In particular, the time-dependent response to reverberation from a simulated linear FM chirp signal is compared for conventional and MVDR beamformers, and for twin-line and crossed-dipole line arrays. The principal conclusions of the study are as follows:

- Under some conditions, conventional limaçon beamforming of the crossed-dipole array provides poorer noise suppression than is attainable with omni-sensor beamforming.
- MVDR-limaçon beamforming provides improved suppression of noise arrivals from conjugate directions, but suffers from signal attenuation in cases of multipath arrivals. It is shown that the latter effect can be reduced by using sub-array averaging.
- Twinned-array MVDR beamforming offers roughly similar performance to that of limaçon MVDR beamforming, but at the expense of more complex processing.

P516763.PDF [Page: 9 of 57]

- If there are no strong azimuthal peaks in the time-evolving reverberation field, MVDR appears to offer little or no improvement in detection performance, as expected.

Significance

This report provides guidance on the potential value of adaptive beamformers that may be considered for use in future LFA towed array sonars. The report also examines the relative merits of single arrays of crossed dipole sensors and twin arrays of omnidirectional sensors, both of which can provide gain selectively against noise or reverberation arriving from one side or the other with respect to the array axis. This work can form the basis of more extensive cost-benefit analyses of various sonar design options. However, the results must be treated with caution until they can be confirmed using real data.

Swingler, D. N. 2001. Adaptive Array Processing in a Wideband Reverberant Environment. DREA CR 2001-120. Division of Engineering, Saint Mary's University.

P516763.PDF [Page: 10 of 57]

Sommaire

Introduction

La réverbération causée par la réflexion d'impulsions de sonars actifs sur les vagues de surface, la topographie sous-marine ou les inhomogénéités de la colonne d'eau constituent habituellement le fond sur lequel les échos de cible doivent être détectés. Les signaux d'un réseau linéaire de capteurs remorqués sont formés en faisceaux afin d'atténuer la réverbération et le bruit de fond et de déterminer la direction de la cible. Le sonar actif basse fréquence (LFA) fonctionne généralement dans une gamme de fréquences qui permet d'incorporer des capteurs à doublets horizontaux au réseau remorqué. Les signaux de ces capteurs peuvent se combiner aux signaux omnidirectionnels pour former des diagrammes de sensibilité directive de type limaçon dans le plan horizontal. Ces configurations peuvent être dirigées vers la gauche ou vers la droite pour résoudre l'ambiguïté directive inhérente aux réseaux rectilignes de capteurs omnidirectionnels. De même, elles peuvent servir à atténuer le bruit parasite ou la réverbération provenant du côté du réseau opposé à la cible. Un autre moyen d'assurer la discrimination gauche/droite consiste à remorquer deux réseaux étroitement parallèles.

Dans de nombreuses conditions, il est possible d'améliorer la discrimination par rapport au brouillage de fond au moyen de conformateurs de faisceaux adaptatifs, dont les poids sont variés afin d'optimiser les critères de performance spécifiés. Toutefois, l'évolution temporelle de la réverbération et la présence de propagation multitrajets au niveau du réseau de réception posent des difficultés qui tendent à détériorer la performance de la plupart des conformateurs de faisceaux adaptatifs. La présente étude fait appel à des simulations pour comparer la performance de conformateurs de faisceaux classiques et de conformateurs adaptatifs ainsi que les types de réseaux linéaires mentionnés ci-dessus dans des conditions de fonctionnement typiques d'un sonar LFA.

Résultats

Le présent rapport examine principalement le conformateur adaptatif MVDR (Minimum-Variance Distortionless Response). En particulier, la réponse temporelle à la réverbération d'un signal chirp linéaire simulé est comparée pour des conformateurs classiques et des conformateurs MVDR, ainsi que pour des réseaux jumelés et des réseaux linéaires à doublets croisés. Les principales conclusions de l'étude sont les suivantes :

- Dans certaines conditions, la formation de faisceaux classiques de type limaçon du réseau à doublets croisés supprime moins bien le bruit que la formation de faisceaux de capteurs omnidirectionnels.

- La formation de faisceaux MVDR de type limaçon améliore la suppression des bruits provenant de directions conjuguées, mais le signal est atténué dans le cas d'arrivées de signaux multitrajets. Le rapport montre qu'on peut réduire ce dernier effet au moyen de la technique d'établissement de moyenne de sous-réseaux (sub-array averaging).

P516763.PDF [Page: 11 of 57]

- La formation de faisceaux MVDR en réseaux jumelés offre une performance à peu près équivalente à celle de la formation MVDR de type limaçon, mais en augmentant la complexité du traitement.

- En l'absence de fortes crêtes azimutales dans le champ de réverbération temporel, le conformateur MVDR semble offrir peu ou pas d'amélioration de la performance de détection, conformément aux attentes.

Importance des résultats

Le présent rapport fournit des orientations en ce qui concerne la valeur éventuelle de conformateurs de faisceaux adaptatifs que pourraient éventuellement utiliser de futurs sonars LFA à réseaux remorqués. En outre, il examine les mérites relatifs de réseaux simples de capteurs à doublets croisés et de réseaux jumelés de capteurs omnidirectionnels, ces deux types de réseaux permettant des gains sélectifs par rapport au bruit ou à la réverbération provenant d'un côté ou l'autre de l'axe du réseau. Ces travaux peuvent constituer la base d'analyses coûts-avantages plus poussées des diverses options de configurations de sonars. Toutefois, les résultats doivent être traités avec prudence jusqu'à ce qu'ils puissent être confirmés par des données réelles.

Swingler, D. N. 2001. Traitement adaptatif applicable à des réseaux dans un environnement réverbérant à large bande. CRDA CR 2001-120. Division of Engineering, Saint Mary's University.

P516763.PDF [Page: 12 of 57]

Table of contents

Abstract i

Résumé i

Executive summary iii

Sommaire v

Table of contents vii

1. Introduction 1-1

2. MVDR experiments in connection with a limaçon line array 2-1
   - 2.1 Introduction 2-1
   - 2.2 A reverberant scenario simulator 2-1
   - 2.3 Beamforming strategies with a single line array 2-3
     - 2.3.1 The basic delay-and-sum beamformer (CB) 2-3
     - 2.3.2 The classic MVDR with omni-sensors only (MVDR) 2-3
     - 2.3.3 Delay-and-sum with fixed limaçon weights (CB_LIM) 2-4
     - 2.3.4 MVDR with fixed limaçon weights (MVDR_LIM) 2-5
   - 2.4 Experimental results 2-5
   - 2.5 Some further experiments 2-6
   - 2.6 Summary 2-8

3. MVDR beamforming with a line array of limaçons: The problem of quasi-simultaneous chirp arrivals 3-1
   - 3.1 Introduction 3-1
   - 3.2 The mathematical model 3-1
   - 3.3 The problem of simultaneous chirp arrivals 3-3
   - 3.4 Numerical examples 3-5
   - 3.5 A partial solution to the cancellation problem 3-8
   - 3.6 Summary 3-9

P516763.PDF [Page: 13 of 57]

4. MVDR beamforming using two parallel arrays 4-1
4.1 Introduction 4-1
4.2 Some numerical examples 4-1
4.3 Summary 4-4

5. Some elementary detection statistics 5-1
5.1 Power measurements 5-1
5.2 SNR analysis 5-1
5.3 Deflection factor calculations 5-2
5.4 Summary 5-3

6. Conclusion 6-1

P516763.PDF [Page: 14 of 57]

1. INTRODUCTION

In this report we are concerned with the performance of adaptive wideband processing schemes suitable for active sonar in a highly reverberant environment. In particular, one of main areas to be examined is the ability to deal with interferences emanating from the so-called conjugate angle. For a horizontal line array electronically steered to an angle, θ_0, with respect to broadside, it is unavoidably steered simultaneously to the conjugate angle, π-θ_0. This is otherwise known as the forward/backward ambiguity for a line-array. A second more general area investigated is that of the advantages of using Minimum-Variance Distortionless Response (MVDR) principles in the adaptive beamformer.

The primary beamforming schemes chosen for investigation are: (1) a limacon array, where each limacon sensor comprises a small dipole normal to the array axis together with a co-located omni-sensor, the weights of which can be (non-adaptively) tuned to provide unity gain in the desired direction and zero gain (i.e a null) in the conjugate direction; (2) a MVDR extension to this approach where the limacon outputs are themselves weighted according to an MVDR scheme where the weights are those which minimise the overall output energy measured over some suitably chosen time interval; (3) a horizontally twinned parallel pair of identical line-arrays of omni-sensors where the sensor weights are again given by a MVDR approach. For completeness we also compare the performance of a conventional (delay-and-sum) beamformer and a basic MVDR beamformer both based on a uniform line-array of omni-sensors. These beamformers are identified by the acronyms, CB_LIM, MVDR_LIM, 2L_MVDR, CB, MVDR respectively, forming five beamformers in all.

The signal is assumed to be a linear FM chirp and the reverberation background is formed from a sum of similar chirps with random times and directions of arrival. Each beamformer has, in each sensor channel, a filter (or correlator) matched to the known chirp to provide SNR gain against the reverberant background (and any white noise which might be included in the simulation) together with pre-steering (i.e. delaying) the data stream so that arrivals from a chosen steering (or beam) direction are time aligned across all sensor channels. The overall output is the sum of the sensor channel streams. The beamformers differ only in the multiplicative weights which are associated with each sensor.

P516763.PDF [Page: 15 of 57]

Another avenue to be explored is that of the effectiveness of the adaptive processors in dealing with evolving reverberation backgrounds. For instance, in the bistatic case, with a pinger at some point in the field, the early reverberation arrivals will tend to come from the vicinity of the pinger, whereas the later ones will be from a spatially more diffuse angular distribution.

For simplicity, and to reduce the complexity of the software simulations, the output of only one beam is explored in detail and the field structure is assumed to be 2-D. However, it is not felt that this is unnecessarily restrictive.

In Section 2 we start with an investigation of the performance of the CB, MVDR, CB_LIM and MVDR_LIM beamformers in a rapidly evolving reverberant background. In Section 3 we concentrate on a potential deleterious situation where we have a strong mutipath arrival more or less time-coincident with the desired signal. In this situation we show how there can be significant cancellation of the signal. We also demonstrate how sub-array averaging, borrowed from the narrowband MVDR arsenal, is useful in ameliorating this effect. In Section 4 the twinned-array concept is examined and the issue of whether it is beneficial to use quiescent (non-adaptive) nulling in the conjugate direction is addressed. In Section 5 there is a brief investigation into the quantitative issue of SNR gain and deflection factor calculations for each of the beamformers.

Finally, the report concludes with a brief overview in Section 6.

P516763.PDF [Page: 16 of 57]

2. MVDR EXPERIMENTS IN CONNECTION WITH A LIMACON LINE-ARRAY

2.1 Introduction

This section deals with some MVDR-related experiments in connection with a line-array of limacon beamformers. Each limacon comprises a co-located omni-sensor and a small horizontal dipole whose axis is normal to the line of the array. If θ is the azimuth angle of a source in the horizontal plane, measured relative to array broadside, then each dipole has a (horizontal) response proportional to $\cos(\theta)$. To form a limacon we add a weighted version of the dipole output to a weighted version of the corresponding omni to form the limacon response to a source at θ proportional to $(a + b \cos(\theta))$. The omni and dipole weights are thus a, b, respectively. We further assume that for the nth limacon sensor in the line-array we have another "overall" multiplicative weight, w_n, so that the final beamformer output time-series, s(t), from an N-sensor array, is of the form

$$s(t) = \int_{\theta=0}^{2\pi} \sum_{n=1}^{N} w_n (a_n + b_n \cos\theta) g_n(t,\theta)\, d\theta \qquad (2.1)$$

where $g_n(t,\theta)$ represents the time-angle response to the acoustic waveform impinging on the nth sensor. It may include any filtering and/or delays impressed on the raw sensor outputs. The thrust of this entire report lies in examining various adaptive methods of computing the various weights, w_n, a_n, b_n in reverberant scenarios.

2.2 A reverberant scenario simulator

We use MATLAB to simulate a simple 2-D reverberant, plane-wave environment as follows.

1. Create a basic linear FM chirp waveform with predetermined values for: sampling rate, or clock frequency; sweep-rate; duration; and initial frequency.

2. At each new clock tick let there commence the arrival of a new received chirp at sensor #1. Let it have a random phase shift [0, 2π] and a random azimuth angle of arrival, θ. By using a predetermined sensor spacing, speed of propagation etc, create the corresponding delayed/advanced versions of this chirp at the other sensors. For the output of each unity gain omni we simply add this new chirp contribution to any signal samples already existing at these sample times due to previous arrivals. For each dipole's output we multiply the new chirp contribution by the cosine of its angle of arrival prior to its summation with other chirps.

In order to produce a meaningful simulation of the reverberant background, the random angles of arrival are uniformly distributed over an angular interval that typically increases as time progresses. (Note: t=0 is assumed to coincide with the earliest chirp arrival at the array). The function used implies a random angle of arrival $\theta(t)$ uniformly distributed over [$-\theta max(t)$, $+\theta max(t)$] where $\theta max(t)=MAX(\pi t/T, \pi)$. This simply states that the range of arrival angles increases linearly with time until t=T where the distribution becomes 2-D isotropic. This is roughly consistent with a pinger at broadside. The early arrivals will tend to arrive from broadside but the later reverberations will tend to be 2-D isotropic.

For simplicity in this model we keep the amplitudes of the arriving chirps constant whereas in the real world we would expect short term random variations together with an overall decay in received signal strength as time progresses and the reverberation dies out.

In summary, the reverberation background is created from a series of identical overlapping chirps, each from a randomly different direction and with a different phase angle and these are added to form the omni outputs. For the dipole outputs there is an additional weighting of each chirp by the cosine of its arrival angle as discussed above. To each sensor's time-series we may add white noise to simulate self-noise at each sensor.

Signal and interference chirps may be superimposed on this background at predetermined times and angles.

P516763.PDF [Page: 18 of 57]

3. Pass both time-series from each sensor (omni and dipole) through a matched filter (matched to the basic chirp) to provide discrimination against the background reverberation and white noise. These matched filters are also known as correlators.

4. Chose a beam (or look, or steering) direction and insert a delay at each sensor to temporally align any signals emanating from the chosen beam (or look, or steering) direction. Steps (3) and (4) are both simply and simultaneously accomplished by frequency domain techniques based on the FFT. We utilise only the positive temporal frequency components; the negative ones are discarded. This implies the output time-series are complex.

5. Take L consecutive points from the complex, matched-filter output time-series (both omni and dipole) at each sensor location and subdivide these into M-point contiguous sub-series. For each M-point sub-series, use MVDR-based methods to find "optimum" values for the weights, w_n, a_n, b_n as indicated in equation (2.1).

Various strategies for computing the w_n, a_n, b_n weights are discussed below.

2.3 Beamforming strategies with a single line array.

2.3.1 The basic delay-and-sum beamformer (CB).

The benchmark for our beamformer is the classic delay-and-sum approach. As we have already performed the necessary delays in Step 4 above, we simply add the N omni-sensor outputs to form the final beam output in the chosen steering direction with unity gain. In this case $w_n = 1/N$, $a_n = 1$, $b_n = 0$.

2.3.2 The classic MVDR with omni's only (MVDR) .

If we set $a_n=1$ and $b_n=0$ then we have the familiar MVDR beamformer in which the weights w_n , operating only on the omni-sensors, are computed adaptively for each

M-point sub-interval. If we write the M-point, pre-steered, matched filter output time-series samples from the nth omni sensor as the M by 1 vector $\mathbf{f}_n$ and use it as the nth column of the M by N matrix **F**, then the pre-steered, fully adaptive, unity gain MVDR (N-1 degrees of freedom) is given by the weight vector **w** where

$$\mathbf{w} = \hat{\mathbf{R}}^{-1}\bar{1} / (\bar{1}^{H}\hat{\mathbf{R}}^{-1}\bar{1}) \qquad (2.2a)$$

and where the N by N sample covariance matrix is given by $\hat{\mathbf{R}} = \mathbf{F}^{H}\mathbf{F}$ and $\bar{1}$ is an N by 1 vector of one's, which represents the steering vector in this pre-steered scenario.

In this work, we use a more general, partially adaptive MVDR with fewer than N-1 degrees of freedom (DOF). This improves the misadjustment situation for our short-time processor. The weight vector is given by

$$\mathbf{w} = \mathbf{w}_0 - \mathbf{C}^{H}(\mathbf{C}\hat{\mathbf{R}}\mathbf{C}^{H})^{-1}\mathbf{w}_0 \qquad (2.2b)$$

where $\mathbf{w}_0$ is the quiescent weight vector, here $\bar{1} / N$, which is recognised as being equivalent to the conventional beamformer (CB) weights. In (2.2b) **C** is a DOF by N blocking matrix where each row is orthogonal to the steering vector, $\bar{1}$.

2.3.3 Delay-and-sum with fixed limacon weights (CB-LIM)

The above methods have no means of resolving the front/back ambiguity inherent in a line-array of omni sensors. However, the limacon does offer forward/backward discrimination as follows: Suppose the azimuth steering direction is θ_o. The basic line-array is also unavoidably steered to the "conjugate angle", π-θ_o. In a limacon, however, we have a response in the steering direction of $(a + b\cos(\theta_o))$ and in the conjugate direction $(a + b\cos(\pi-\theta_o)) = (a - b\cos(\theta_o))$. If we set the former to unity (i.e. unity gain) and the latter to zero (i.e. cancellation) and solve for a, b we get

$$a_n = 0.5, \qquad b_n = 0.5 / \cos(\theta_o). \qquad (2.3)$$

In the delay-and sum limacon beamformer, these limacon outputs are matched-filtered, delayed and summed along the lines discussed above. In this application, $w_n = 1/N$.

2.3.4 MVDR with fixed limacon weights MVDR_LIM)

The limacon outputs of the CB-LIM, after matched filtering and delaying are used to form the MVDR weight vector, $\mathbf{w}$, as described above in Section 2.3.2.

2.4 Experimental Results

Fig. 2.1 shows a typical L=256 point waveform from one of the omni-sensors. The basic chirp is a 32-point FM chirp with frequency rising linearly from 600Hz to 1000Hz. The sampling rate is 2.5kHz. The individual "background" chirps have random angles of arrival and an amplitude of unity except those arriving initially at "sample times" 110, 150 and 210 (in 2500^{-1} = 0.4mS intervals) where the amplitudes are deliberately increased to 5, 25, 25 respectively. The corresponding three angles of arrival are set at $\pi/4$, $-\pi/4$, $3\pi/4$, respectively. These represent the steering (or beam) angle, a jammer angle and the conjugate angle, respectively. The high amplitude bursts with onset times of 150 and 210 are highly visible in Fig. 2.1. The desired signal near 110 is not discernible.

The angle of arrival of the background chirp initially arriving at sample time k>0 is random and uniformly distributed over the interval $(\pi/64)$ [-k , k] for l<64 and uniform over $[-\pi, \pi]$ thereafter. Thus near the beginning of the time series, the chirps all appear to emanate from near broadside. After time k=64 samples, the reverberation tends to be 2-D isotropic. This is consistent with a pinger near broadside.

After passing through the matched-filter (correlator), the waveform magnitudes might be as shown in Fig. 2.2. There are N=8 sensors and all eight sensor outputs are shown superimposed. The compression of the 32-point chirps into sinc's just a few sample wide is obvious near times 150 and 210. The sinc width is about $(1000\text{-}600)^{-1}$ S =2.5mS or about 6 samples. Also obvious near these times is that the sincs are time-delayed across the channels. However, after passing through the delay processor which steers the array to $\theta_0=\pi/4$ we have the results of Fig. 2.3. Here the (undesired) chirp which arrives from the conjugate angle is transformed into a family of sincs, temporally aligned across all the channels at time 210.

Simply summing these matched-filtered and time-delayed time-series yields the delay-and-sum beamformer (CB) output shown as the lower graph in Fig. 2.4. This curve is actually the square-root of average of the instantaneous power outputs, averaged over some 16 realisations of this simulation. The upper curve in Fig 2.4 is the corresponding (averaged) output for the classic MVDR beamformer with a single degree of freedom (DOF=1) and with a sub-series length of M=32. It is worth remarking that the MVDR response peak near 210 is lower than that of the CB method. This effect also applies to the desired signal component at time sample 100 and is actually an undesirable effect. If a fully adaptive MVDR beamformer is used (DOF=7) the peak is even lower. This cancellation effect is not fully understood but might be linked to the multipath problem discussed more fully in Section 3. Note the presence of lower level peaks near samples 110 and 150.

If we now employ the fixed limacon weights mentioned above (equation 2.3) to provide unity gain in the steering direction and cancellation in the conjugate direction, the correlator outputs of Fig. 2.5 ensue wherein it is obvious that the strong but unwanted conjugate arrival near 210 has disappeared.

In the previous examples, both the CB_LIM and MVDR_LIM beamformers have little difficulty in attenuating the strong, but angularly remote, interferer near time 150. The interference suppression potential of the MVDR_LIM approach is more evident in the results of Fig. 2.6 where the jammer is now situated much closer to the steering direction, at $\theta=\pi/8$. This reduces the temporal spread of the jammer response, or alternatively in linear algebra terms, the jammer is more like a rank-1 phenomenon, and the MVDR_LIM beamformer is much more effective in cancelling it than the CB_LIM beamformer. Additionally, the CB_LIM beamformer is more affected due to the amplification of the interference through the influence of the limacon beampattern. Note, as expected, that there is no contribution in Fig. 2.7 relating to the conjugate signal near time 210.

2.5 Some further experiments

In addition to experiments of the type described above, two other beamformers were simulated. In one case the weights w_n were set to unity, and the limacons were set to unity gain in the steering direction. However the "null angle" for the limacons was varied over the interval $[-\pi, \pi]$ in steps of $\pi/6$. The rational here is than any single strong

P516763.PDF [Page: 22 of 57]

jammer, no matter what its angle of arrival, should be largely nulled out by the appropriate choice of null angle and thus the "best" null angle is that which minimises the overall beamformer output energy over the M point sub-series. Unfortunately, if the jammer angle, θ_j, is close to that of the steering direction, i.e. $|\theta_j| \sim |\theta_0|$, this causes large responses elsewhere in the limacon beampattern which brings up the background level to a degree which overwhelms the positive effects of cancelling the jammer. This approach was rejected.

In a second experiment, the weights w_n were again set to unity but the limacon weights a_n, b_n were found from an MVDR energy minimisation approach, subject to an overall unity response of the limacons in the steering direction and an overall cancellation effect in the conjugate direction. i.e. the constraints in matrix form are

$$\begin{bmatrix} \bar{\mathbf{T}}^t & \bar{\mathbf{T}}^t \cos(\theta_0) \\ \bar{\mathbf{T}}^t & -\bar{\mathbf{T}}^t \cos(\theta_0) \end{bmatrix} \begin{bmatrix} \mathbf{a} \\ \mathbf{b} \end{bmatrix} = \begin{bmatrix} 1 \\ 0 \end{bmatrix}$$

where **a**, **b** are the N by 1 vectors containing the a_n, b_n values. For similar reasons as above, this approach was also not considered successful.

In a third experiment, the limacon weights were each fixed to give unity gain in the steering direction and cancellation in the conjugate direction. This in effect forces a known modulation effect (the limacon beampattern) onto the spatial frequency distribution to be processed by any subsequent beamforming. Assuming the true background is spatially white ("unmodulated"), this implies that some "fixed", optimum MVDR weight vector, **w**, can be computed for this modulated, or limacon, situation if we further assume a narrowband scenario running at the mid-frequency of the chirp, or 800Hz in this experiment. However, this seemed to offer negligible improvement over the CB method as the spatial frequency modulation effect is usually quite smooth and the beamformer output power is dominated by the MVDR beampattern in the main lobe region for which the sinc shape is already quasi-optimum. Indeed, in most situations the overall MVDR beampattern was very similar to the CB sinc distribution. Again, then, this approach was rejected as offering negligible advantage over the CB_LIM approach.

Finally, it might be mentioned that the simulation software was modified to include narrowband and wideband (white noise) non-reverberant interferers. However, beyond verifying that both types of interference were attenuated by the beamformers, no

significant effort was made in investigating these scenarios. It should be recalled that the major area of interest in this report lies in reverberant scenarios.

2.6 Summary

The above experiments have revealed the following:

(1) The basic CB beamformer in conjunction with "conjugate nulling" limacons and matched filtering seems competitive in comparison to a single-tap MVDR beamformer used in the same fashion. Both offer forward/backward discrimination; a feature not offered by a line-array of omni-sensors. A potential problem does arise if the steering angle is near endfire $|\theta_o| \sim \pi/2$ as the limacon weight, $b = 0.5/\cos(\theta_o)$ become large, implying very large limacon responses in the forward/backward broadside directions which can swamp the sidelobe response of the subsequent CB beamformer.

(2) The single-tap MVDR method has an advantage where there are strong jammer(s) near the steering direction. In this case the jammer has low rank properties which makes it a candidate for effective MVDR nulling. When the jammer is angularly more remote, its responses are temporally non-aligned across the sensor channels and while the jammer signal it loses its low rank nature, the temporal spreading results naturally in an overall attenuation which might be adequate under many circumstances.

(3) With a M=32 sub-series length, the fully-adaptive MVDR approaches did not perform well for even as few as N=8 sensors. Any attempt to use the fully adaptive MVDR beamformer (DOF=7) led to almost complete cancellation of the desired signal itself, notwithstanding the "unity gain" rationale of the MVDR design philosophy. This would suggest that using more taps in the MVDR processor would not help as this requires even more degrees of freedom in the data. If the sub-series length (M) were increased, then the increased temporal averaging involved would tend to suppress any response to a strong chirp. Balancing these two issues seems to pose an interesting problem.

(4) The MVDR beamformers did not seem able to take significant advantage of the reverberation background which evolved over time. An exception occurs near the very beginning of the time-series where all the signal appears to be emanating from

broadside. In this case the MVDR would null effectively. However, as tine progressed and the reverberation appeared from more off broadside angles, the MVDR did not seem able to usefully take advantage. Again this is probably due to the overall response being dominated by the mainlobe of the overall beampattern for which the CB is quasi-optimum.

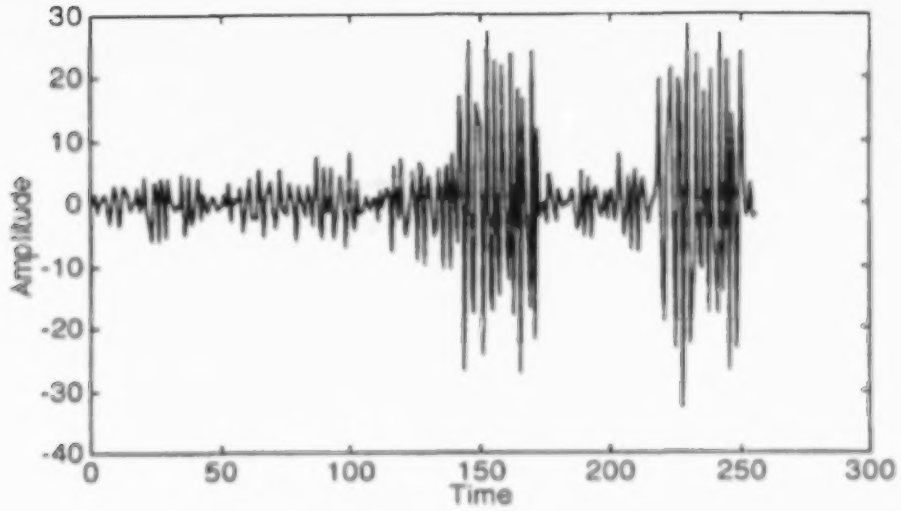

Fig. 2.1 Typical time series from an omni sensor. Note the strong chirps with onset times near time=150 and 210. The former represents a jammer, the latter a strong chirp from the "conjugate" angle. There is weak signal from the desired direction at time=110.

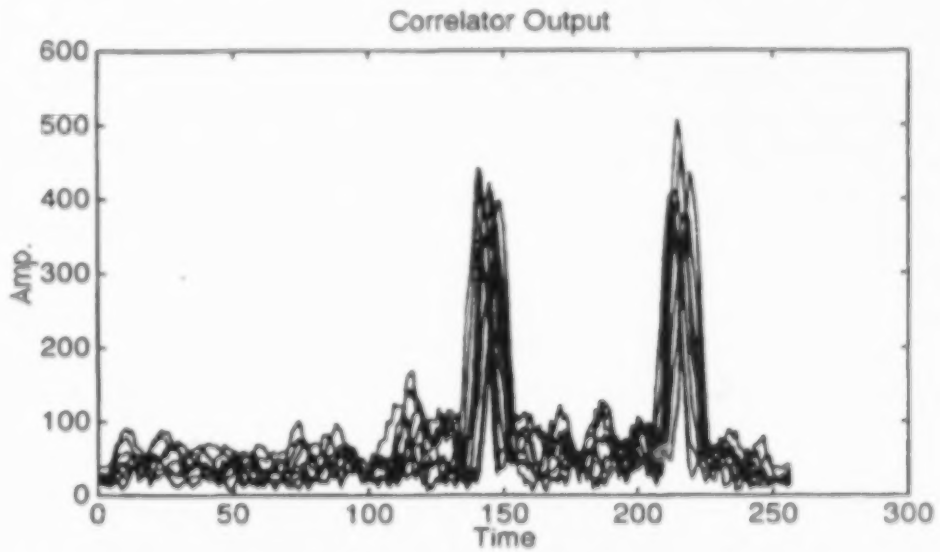

Fig. 2.2 Superimposed outputs of all eight channels after passing through matched-filter. Note strong sinc's near 150 and 210.

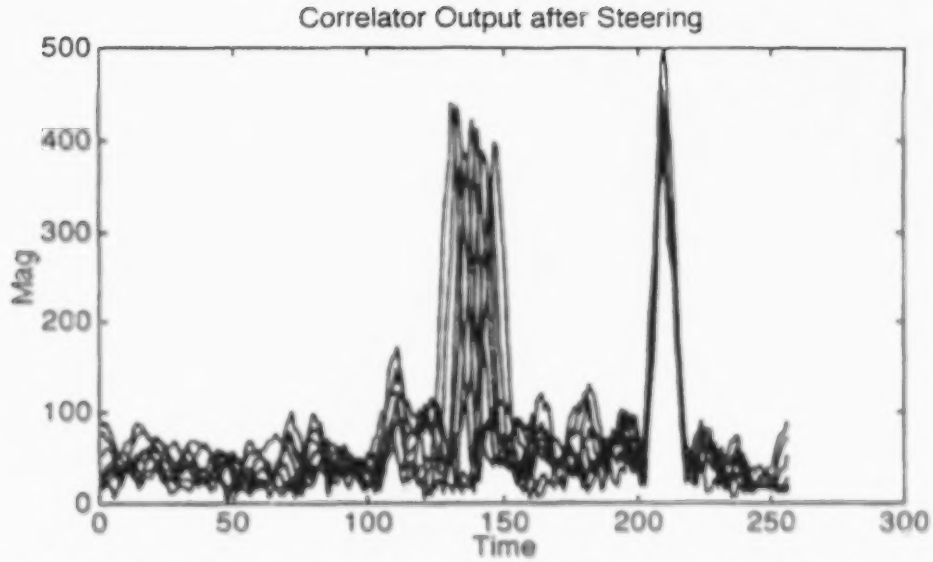

Fig. 2.3. All eight channels after passing through delay units to steer beamformer to desired direction. Note alignment of conjugate sincs at 210, misalignment of jammer sincs near 150.

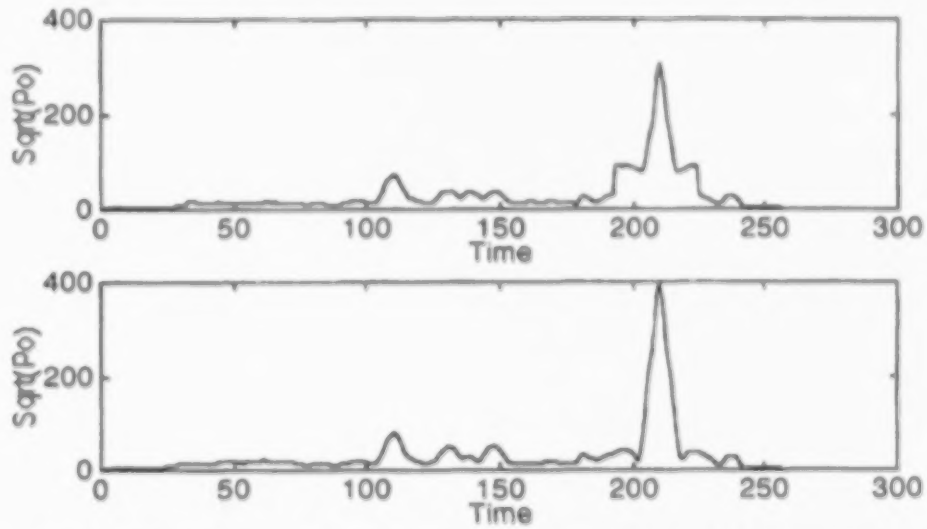

Fig. 2.4. Upper trace: MVDR beamformer output (averaged over 16 realisations).
Lower trace: CB beamformer output (averaged over 16 realisations)

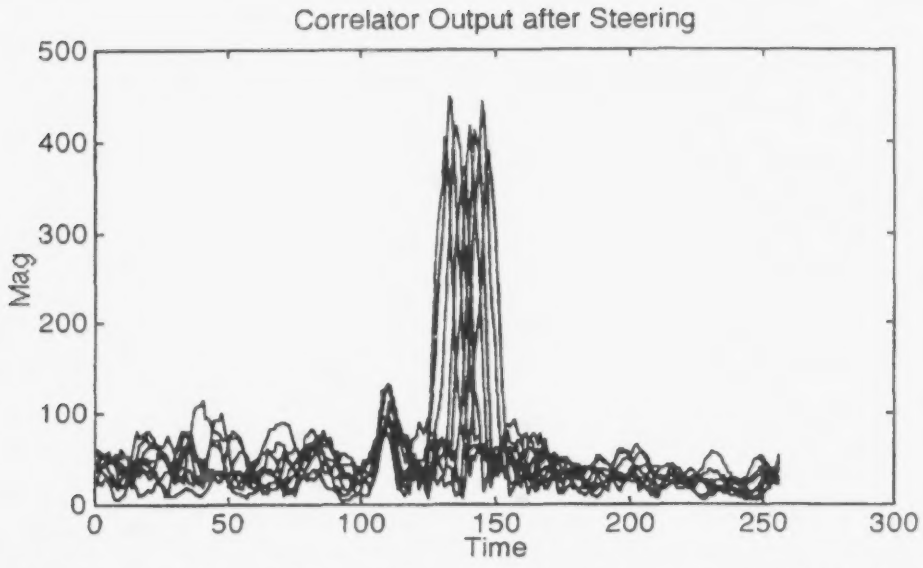

Fig. 2.5. As Fig. 2.3 but with limacons tuned to cancel conjugate arrivals. Note the disappearance of spikes near time = 210.

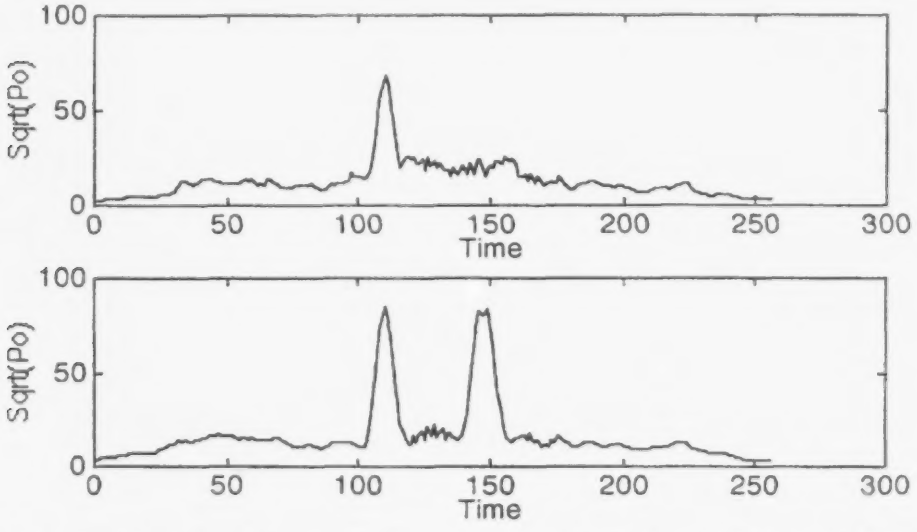

Fig. 2.6. Impact of moving jammer closer to steering direction. Note that the CB_LIM jammer response at 150 is large (lower trace) whereas the MVDR_LIM beamformer (upper trace) attenuates this jammer more strongly. Again note the disappearance of the conjugate arrival near time 120.

P516763.PDF [Page: 28 of 57]

3. MVDR BEAMFORMING WITH A LINE-ARRAY OF LIMACONS: THE PROBLEM OF QUASI-SIMULTANEOUS CHIRP ARRIVALS.

3.1 Introduction

As outlined in Section 2, we consider a line array of limacons upon which impinges a mutipath set of similar chirp waveforms. We assume that a few of these arrivals are dominant (from targets and/or interferers). The limacons are tuned to reject any signals emanating from the bearing "conjugate" to that of the desired, or beam, direction. The limacon outputs are matched-filtered which reduces the long chirps to short sinc-type functions with an SNR gain against the reverberant background (and against white noise, too). Simultaneously, the sensor outputs are pre-steered (by using appropriate delays) so that the responses of the each sensor channel to a signal arriving from the desired (or steering) direction are time-aligned.

This section examines, by means of some further simulation experiments, the degree to which such an arrangement is compromised by the presence of a strong mutipath chirp whose arrival time is more or less coincident with the signal from the desired direction, but whose the angle of arrival (DOA) may be quite remote from that of the signal. In such a case, notwithstanding the rationale behind the MVDR "unity gain" approach, the beamforming operation can result in the almost complete loss of the signal component from the overall output, a highly undesirable effect. The multipath arrival is also largely cancelled, but this is, of course, desirable.

We shall demonstrate that the problem can be largely alleviated by using the sub-array averaging approach as in narrowband MVDR beamforming. However, as in the narrowband case, if the interfering chirp has a DOA quite close to the desired signal, even this approach is not particularly effective.

3.2 The mathematical model

For purposes of simplicity, we shall again assume a 2-D active sonar model based on a uniform line-array of limacons. The background field is highly reverberant and comprises multipath echoes of the primary chirp arriving from M (>>1) different bearings at different times. Hence the time-domain output of the nth sensor might be written as

P516763.PDF [Page: 29 of 57]

$$u_n(t) = \sum_{m=1}^{M} A_m B(\theta_m) g(t - t_m - (n-1)\tau_m) e^{j\phi_m} \tag{3.1}$$

where

A_m is the amplitude of the mth chirp
$B(\theta_m)$ is the overall limacon gain for the mth chirp at bearing angle θ_m
t_m is the arrival time of the mth chirp measured at the 1st sensor
τ_m is the inter-sensor delay for the mth chirp
g(.) is the complex analytic version of the bandpass chirp signal
ϕ_m is a random phase shift undergone by the mth chirp.

It is easier to move into the frequency domain where (3.1) is rewritten as

$$U_n(\omega) = \sum_{m=1}^{M} A_m B(\theta_m) G(\omega) e^{-j\omega t_m} e^{-j\omega(n-1)\tau_m} e^{j\phi_m} \tag{3.2}$$

This signal is passed through a matched filter with frequency response $G^*(\omega)$ and, simultaneously, beam-steering is achieved by inserting a time delay of $(n-1)\tau_0$ where τ_0 is the inter-sensor delay associated with the chosen beam (or steering) direction. Thus the output after matched filtering, also known as the correlator output, and steering is given by

$$V_n(\omega) = \sum_{m=1}^{M} A_m B(\theta_m) |G(\omega)|^2 e^{-j\omega t_m} e^{-j\omega(n-1)(\tau_m - \tau_0)} e^{j\phi_m} \tag{3.3}$$

Moving back into the time domain we have

$$v_n(t) = \sum_{m=1}^{M} A_m B(\theta_m) \Phi_{gg}(t - t_m - (n-1)(\tau_m - \tau_0)) e^{j\phi_m} \tag{3.4}$$

where $\Phi_{gg}(t)$ is interpreted as the autocorrelation function of the basic chirp signal, $g(t)$. Equation (3.4) simply states that the output of the mth channel, after correlation and steering, is given by the weighted sum of delayed auto-correlation functions.

P516763.PDF [Page: 30 of 57]

In order to calculate the MVDR_LIM weights, we next compute an estimate of the N by N covariance matrix, *R*, estimated over some time interval of length T with the pqth entry as follows :

$$R_{pq}(t,T) = \int_{t}^{t+T} v_p(t)\, v_q^*(t)\, dt \tag{3.5}$$

From (3.4), (3.5) the expected value of R_{pq} for the background reverberation is approximately

$$R_{pq}(t,T) = ME(A_m^2)\, E\left(B^2(\theta)\right) \sum_m \tilde{\Phi}((p-q)(\tau_m - \tau_0)) \tag{3.6}$$

where $\tilde{\Phi}$ represents the autocorrelation function Φ_{ss}. The product $ME(A_m^2)$, $M \to \infty$, is interpreted as a measure of the background chirp noise variance at the output of an omni-sensor. If we make the assumption that the spectrum $G(\omega)$ of the chirp is rectangular and of width $\Delta\omega$ centred on frequency ω_0, then we might very approximately write (3.6), after dropping unnecessary multiplicative constants as

$$R_{pq}(t,T) = E\left(B^2(\theta)\right) \mathrm{sinc}((p-q)\Delta\omega d / 2c) \cos((p-q)\omega_0 d / c) \tag{3.7}$$

where d is the inter-element spacing and c is the speed of propagation. The last two factors on the right essentially comprise the coherence function of the reverberant background.

Once **R** is computed, the N MVDR_LIM weights can be computed according to (2.2a) or a reduced-DOF version of it (2.2b).

3.3 The problem of simultaneous chirp arrivals

Suppose we have a desired chirp of amplitude A_0 arriving at t_0 with phase angle θ_0 and an interfering chirp of amplitude A_1 arriving at t_1 with phase angle θ_1 from a bearing with inter-element delay τ_1. The signal and interference sum from the nth steered correlator channel can be written as

$$y_n(t) = A_0 B(\theta_0) \Phi_{ss}(t - t_0) e^{j\phi_0} + A_1 B(\theta_1) \Phi_{ss}(t - t_1 - (n-1)(\tau_1 - \tau_0) e^{j\phi_1} \tag{3.8}$$

P516763.PDF [Page: 31 of 57]

Regarding these two in isolation, their covariance matrix contribution R_{pq} is given by

$$R_{pq} = \int y_p(t) y_q^*(t) dt \tag{3.9}$$

R_{pq} is highly dependent on the relative delay t_1-t_0. If this is large (i.e. greater than about 1/bandwidth_of_chirp) then the two sinc-like components in (3.8) are temporally well separated and we have roughly, to within an unimportant multiplicative constant,

$$R_{pq} = A_0^2 B^2(\theta_0) + A_1^2 B^2(\theta_1) \tilde{\Phi}((p-q)(\tau_1 - \tau_0)) \tag{3.10}$$

where we assume $\tilde{\Phi}(0)=1$. Equation (3.10) can be simplified on recognising that $B(\theta_0)=1$ by design. If τ_1 and τ_0 are not too close (i.e. not similar bearings) then the signal and interference contributions to the covariance matrix are linearly independent and they act as if uncorrelated.

However, if the relative delay is small, then t_1-t_2 = 0, approximately, and (3.9) becomes

$$R_{pq} = A_0^2 B^2(\theta_0) + A_1^2 B^2(\theta_1) \tilde{\Phi}((p-q)(\tau_1 - \tau_0))$$

$$+2B(\theta_0) B(\theta_1) \Re e(A_0 A_1 e^{j\phi_0} e^{-j\phi_1} \tilde{\Phi}((p-q)(\tau_1 - \tau_0))) \tag{3.11}$$

The third term on the right immediately shows that the signal and interference terms are coupled and can no longer be regarded as independent. As a result, this allows the MVDR beamformer, in keeping with its energy minimization philosophy, to attempt to cancel both the signal and interference components simultaneously (without violating the unity gain signal constraint).

In general signal cancellation occurs if both the interference and signal components are strong (relative to the background) in the same temporal region. Thus the problem will most likely arise if the signal and interference are both strong and have similar (i.e. within the reciprocal of the chirp bandwidth) arrival times. It is not necessary for the bearings to be similar.

In the following examples, we will demonstrate the above effect. Further, by borrowing the technique of sub-array averaging from the narrow-band MVDR method, we shall show how the negative impact can be ameliorated, provided the bearings of signal and interferer are not too close.

3.4 Numerical examples

For the purposes of this section we shall again consider a 2-D model with a desired signal angle (relative to broadside) of 0.45π. There exists a strong chirp signal of amplitude A_0=30 at this bearing and an interference chirp of similar strength whose arrival angle and times will be varied. A second eqi-strength interferer is placed at the "conjugate" angle for a regular line array, i.e. at π-0.45π=0.55π.

As mentioned in the previous Section, the reverberant background is simulated by ensuring that at each sample time a new background chirp impinges on the array. In the current experiments the background arrival bearings are uniformly distributed over $[0,2\pi]$. Each has unity amplitude but a randomised phase shift.

Again the simulation is based on a linear FM chirp with 400Hz bandwidth centred on 800Hz. The chirp is 32 samples in length (sampling rate =2.5kHz) so 32 chirps with randomised phases overlap at each sample point. Hence, the reverberant background noise power is 32 units and the sensor level SNR for the signal and interferer(s) is roughly 10log(900/32)=14.8dB, at the hydropohone level.

We recall that the limacon beampattern $B(\theta)$ is given by

$$B(\theta) = a + b\cos(\theta)$$

so after passing through the limacon the background noise power will be $32\,E(B^2(\theta)) = (32/2\pi)\int_0^{2\pi} B^2(\theta)\,d\theta = 32(a^2 + b^2/2)$. In our case, with the steering direction set at 0.45π, we have a=0.5, b=3.2 so the average reverberation background power, post-limacon, is about 32*(0.25+3.2^2/2)=172 and the corresponding SNR for the (unity gain) signal is about 10log(900/172)=7.2dB. However, the limacon gain for the interferer depends on its bearing angle, θ_1, and the interference INR will be $7.2+20\log(B(\theta_1))$ dB.

P516763.PDF [Page: 33 of 57]

For the interferer at the conjugate angle, we have $B(\theta_{conj})=0$ by design, and consequently this interferer plays no further role in the processing stream.

Fig. 3.1(a) shows a typical (post-limacon) output time-series measured over 256 samples from Sensor #1 for an N=8 sensor array with inter-element spacing of 0.8m. The speed of propagation is 1500m/s. Recall the sampling frequency is 2.5kHz. The arrival times of the signal, interferer and conjugate interferer are 100, 150, 210 (in sampling units of 1/2500s), respectively. The interferer is angularly quite close to the desired signal, at $\theta_I=0.35\pi$. The signal chirp and one interference chirp are quite visible in Fig. 1(a). Note that the interference chirp arriving at time 150 is about twice as strong as the signal chirp at time 100 due to the impact of the limacon gain. Also note that, as expected, there is no trace of the interference chirp at time 210 from the strong interferer at the conjugate angle. It is nulled out by the limacon action.

In Fig. 3.1(b) we superimpose the envelopes of the output time-series from all eight channels after matched-filtering and pre-steering in the signal direction. It is obvious that the signal chirp at time 100 has been transformed into a family of time-aligned sinc-type functions. As the interferer at time 150 has an arrival angle quite close to that of the signal, its sinc's are also fairly well aligned around time 150.

These eight time-series are then used to build the covariance matrix estimate along the lines of (3.5). From this the eight MVDR weights are calculated, here with five degrees-of-freedom (DOF=5). Finally the eight time-series are combined according to the MVDR weights and this is the final MVDR beamformer output.

In Fig. 3.1(c) we show (solid line) the square-root of the average power output from the MVDR where the averaging is done over eight realisations of the this process. This final averaging is simply to allow the eye to pick out the salient features more easily. For comparison purposes we also show the corresponding output (dashed line) from a conventional (delay-and-sum) beamformer (CB) applied to the same time series. In essence, the conventional beamformer output is simply the average of the N=8 steered-correlator output time-series. Equivalently, it is the MVDR beamformer where the weights are identical and of value (1/N).

Comparing the two curves in Fig. 3.1(c), we note that the signal components are very similar, with the MVDR_LIM response being slightly lower than the CB_LIM.

PS16763.PDF [Page: 34 of 57]

However, in the region of the interference (around sample time 150) we note that the MVDR_LIM beamformer has largely cancelled it out, whereas the CB_LIM beamformer has a very large response to the interferer - indeed larger than the signal response - as its arrival angle falls inside the mainlobe of the CB_LIM beampattern. In passing, we also note that the mean background level in the MVDR_LIM beamformer is slightly elevated in comparison to the CB_LIM. This is a typical effect for a MVDR beamformer attempting to null-out a closely spaced (in angular terms) interferer.

We now move the interferer further from the look-direction and situate it at broadside (θ_I=0). The outputs from the steered correlators are shown in Fig. 3.2(a) where we note that the response to the interference is noticeably "smeared out" over time across the channels, i.e. the time-alignment property is lost. The individual interference responses are greater than those of the signal by a factor of about a+b=3.7, due to the limacon gain. This is the maximum possible limacon gain for a steering angle of 0.45π. The beamformer outputs are shown in Fig. 3.2(b) where we notice again that the MVDR beamformer has effectively cancelled the interference around time 150. The CB_LIM has residual interference effects due to the sidelobe structure in its beampattern. As the MVDR_LIM beamformer is not particularly challenged in this scenario, the background noise levels for the two beamformers are comparable.

Moving the interferer to $\theta_I=-0.35\pi$ yields the results of Fig. 3.3. In Fig.3.3(a) we note even more "smearing" of the interference response across the channels and in Fig. 3.3(b) we note residual interference effects for both beamformer outputs. In the MVDR case, the interference is more difficult to suppress if the smearing is large and there is little time-overlap of the individual interference responses across the channels.

Having established a general superiority in terms of interference suppression for the MVDR_LIM beamformer where there is negligible time-overlap between the signal and interference responses, we move on to examine a case where significant time-overlap does occur. Fig. 3.4(a) shows the steered correlator outputs similar to Fig. 3.1(b) but where the interferer arrives at time 101, not 150. In Fig. 3.4(a) it is impossible to distinguish signal effects from interference effects. However, the beamformer outputs, Fig. 3.4(b), are very different to Fig. 3.1(c) as the MVDR_LIM beamformer almost entirely cancels both signal and interference effects; this is highly undesirable. On the other hand the CB_LIM passes both.

P516763.PDF [Page: 35 of 57]

As seen in Fig. 3.4(c), moving the interferer out from 0.35π to broadside does little to improve the situation for the MVDR_LIM beamformer, while the CB_LIM does reject much of the interference via its sidelobe action. Moving the interferer even further out to $\theta_I = -0.35\pi$ still does not fully eliminate the problem for the MVDR_LIM beamformer, though the effect is less dramatic (see Fig. 3.4(d)).

We are thus left with empirical evidence to support our earlier discussion that quasi-simultaneous arrival of signal and interference can cause significant signal cancellation, irrespective of the interferer's bearing.

3.5 A partial solution to the cancellation problem

A similar problem of signal cancellation arises in the narrow-band MVDR case in the presence of multipath effects. A common approach to reducing its impact involves sub-array averaging to decorrelate the desired and multipath components. From a mathematical perspective, it is equivalent to forming a final N' by N' covariance matrix ($N' \leq N$) as the sum of the individual N' by N' covariance matrices available from each of the N-N'+1 subarrays each of length N' formed from the original N-element array. In our approach this yields N' weights for the MVDR_LIM beamformer which, for simplicity, we apply to the first N' sensor channels.

In Fig. 3.5(a) we rerun the scenario of Fig. 3.4(c) with the interferer arriving at time 101 and at broadside but we now also use sub-array averaging with N' = 6. The MVDR beamformer output of Fig. 3.5(a) appears to suffer much less cancellation and Fig. 3.5(a) is reminiscent of Fig. 3.2(b) where there is no time overlap of the signal and interference.

However, if we move the interferer to within the CB_LIM mainlobe, it is considerably more difficult to introduce significant decorrelation by sub-array averaging. For instance, Fig. 3.5(b) shows the beamformer outputs where the interferer is at 0.35π and where we have N'=6 again. Although the signal cancellation is not as complete as the corresponding case in Fig. 3.4(b), there is still significant cancellation. On the other hand, moving the interferer out to -0.35π results in the beamformer outputs of Fig. 3.5(c) where little cancellation occurs, though there is remnant interference visible to the left of the main peak at time 100.

P516763.PDF [Page: 36 of 57]

Overall, then, we have demonstrated that decorrelation of signal and interference with simultaneous arrival times is possible through the sub-array averaging processing, provided the interference is not too close in angular terms to the desired signal. The results we have demonstrated are largely consistent with those obtained from narrow-band multipath studies

3.6 Summary.

It has been demonstrated that MVDR beamforming in a highly reverberant environment is possible with a line-array of limacons and chirp signals. These limacons are tuned to give unity response in the beam (or steering) direction and a null response in the direction "conjugate" to the steering direction. In the absence of the limacons, signals from such conjugate bearings would be passed with unity gain, too. A potential problem of signal cancellation was identified in connection with quasi-simultaneous arrivals of strong signal and interference chirps. The problem was shown to be significantly reduced by using the concept of sub-array averaging.

P516763.PDF [Page: 37 of 57]

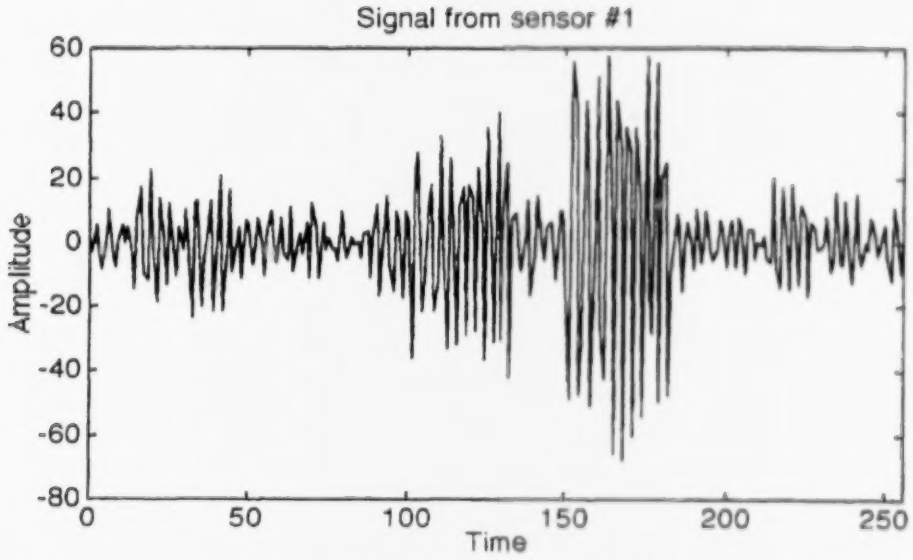

Fig. 3.1(a) Typical output time-series from limacon. A_0 =30, θ_0= 0.45π, t_0 = 100; A_1=30; A_1 =30, θ_1= 0.35π, t_1 = 150; A_2 =30, θ_2= 0.55π, t_2= 210.

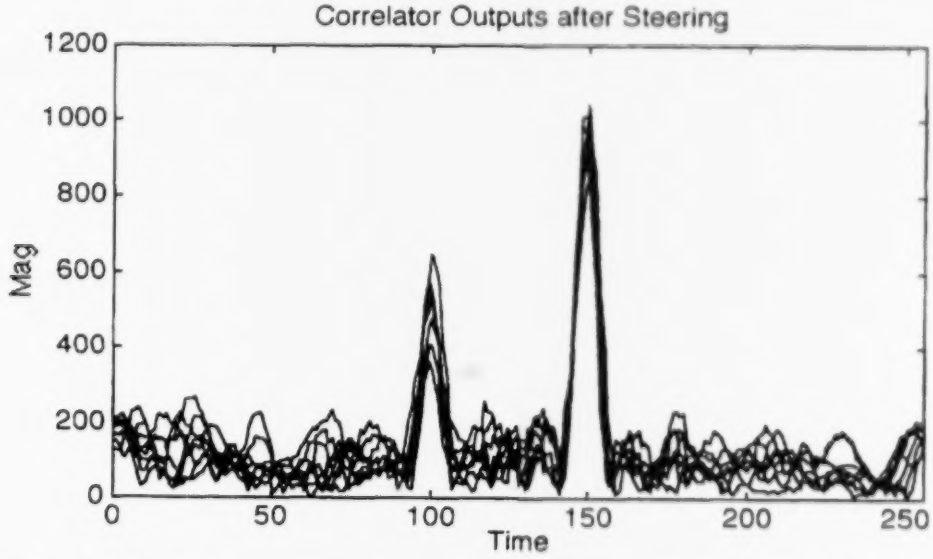

Fig. 3.1(b) As Fig. 3.1(a) but after matched-filtering and steering (Superposition of N=8 channels)

P516763.PDF [Page: 38 of 57]

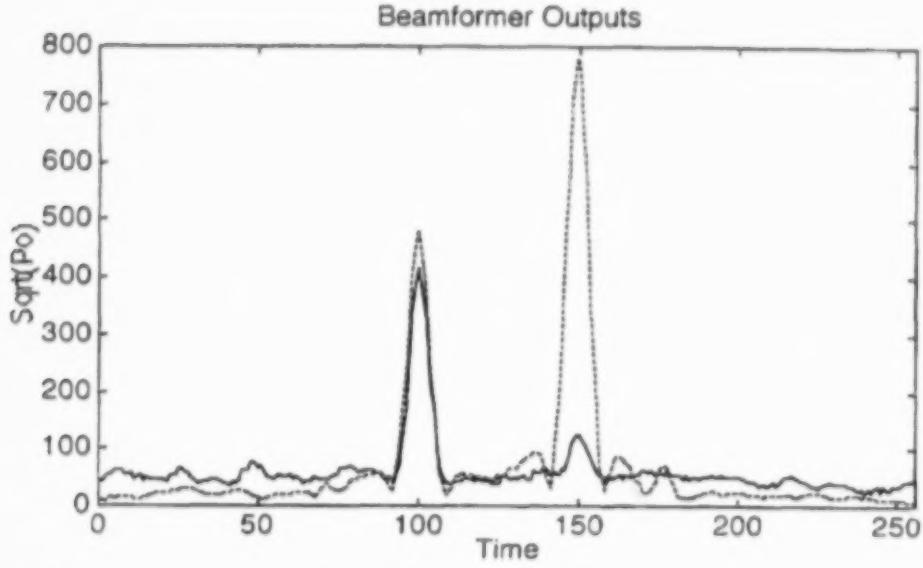

Fig 3.1(c) Output from limacon beamformers (Averaged over eight realisations)
Solid line = MVDR_LIM with 5 DOF; dashed line = conventional beamformer (CB_LIM)

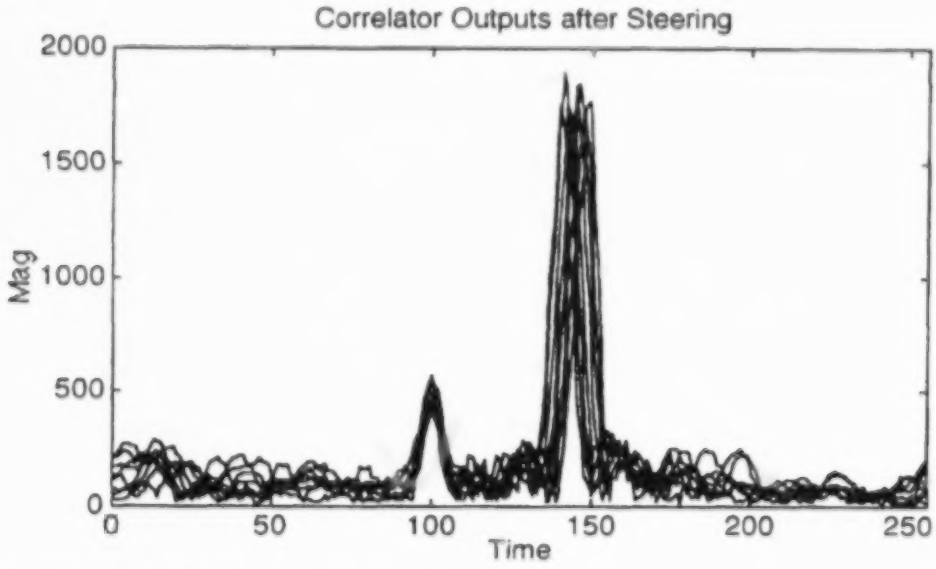

Fig. 3.2(a) As Fig 3.1(b) but with $\theta_2 = 0$ (broadside).

P516763.PDF [Page 39 of 57]

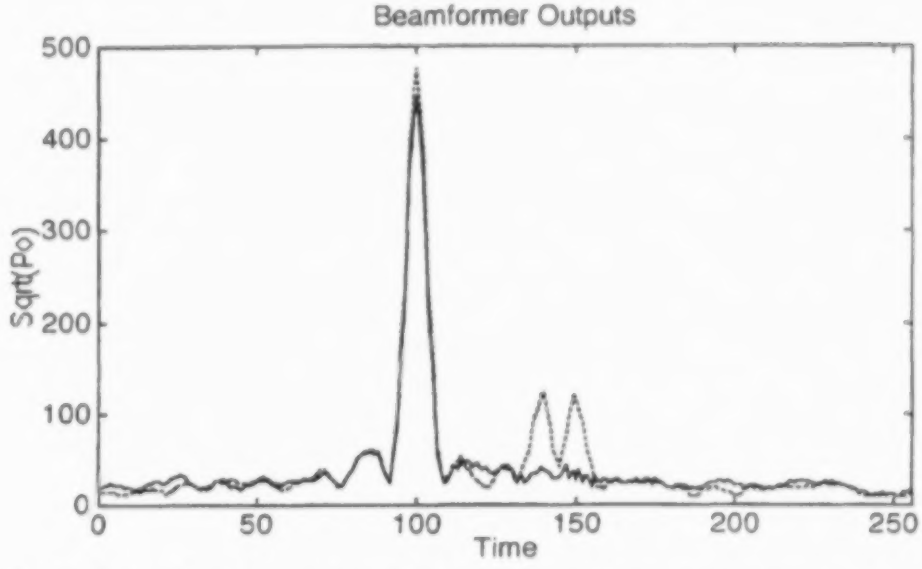

Fig. 3.2(b) Output from limacon beamformers (Averaged over eight realisations) Solid line = MVDR_LIM with 5 DOF; dashed lined = conventional beamformer (CB_LIM)

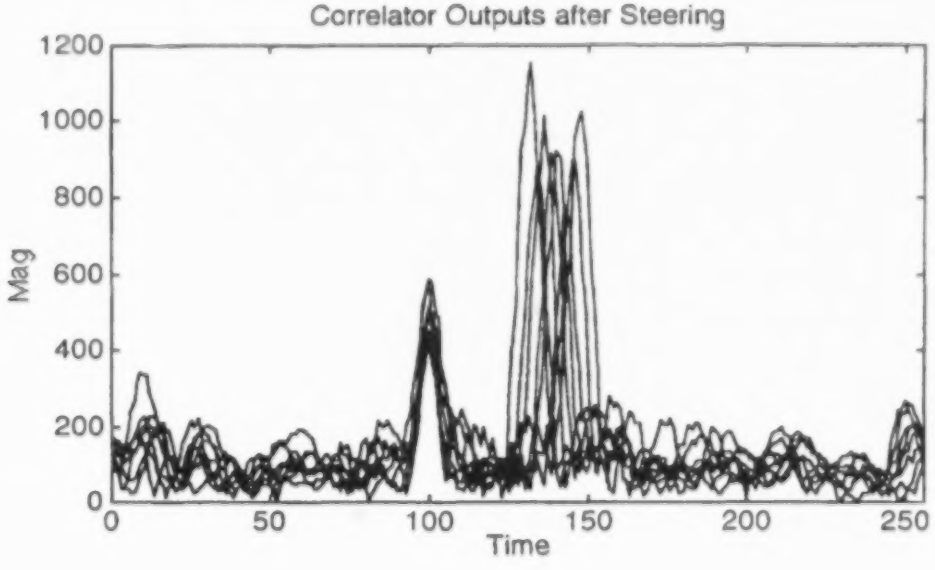

Fig. 3.3(a) As Fig. 3.1(b) but $\theta_1 = -0.35\pi$. Note the spreading of the interference responses near time 150.

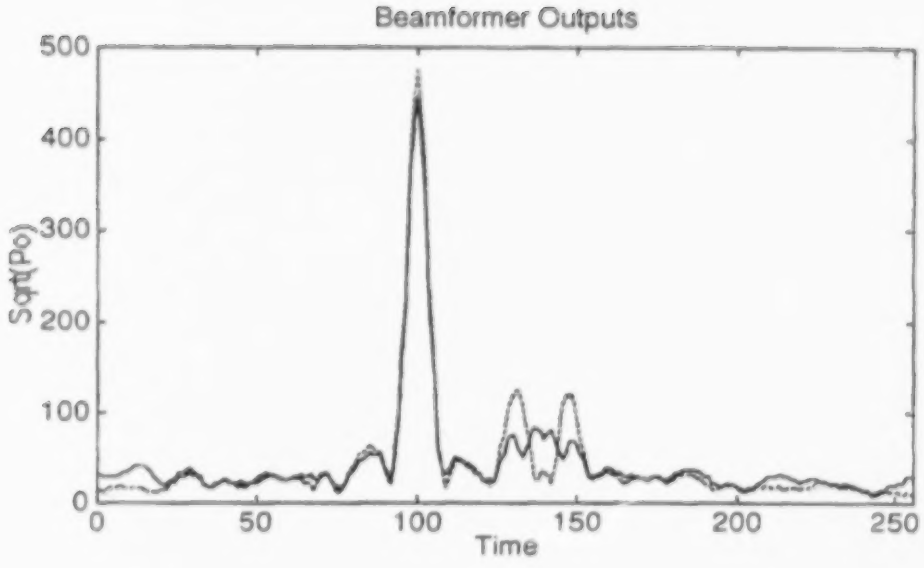

Fig. 3.3(b) Output from limacon beamformers. (Averaged over eight realisations). Solid line = MVDR_LIM with 5 DOF, dashed lined = conventional beamformer (CB_LIM)

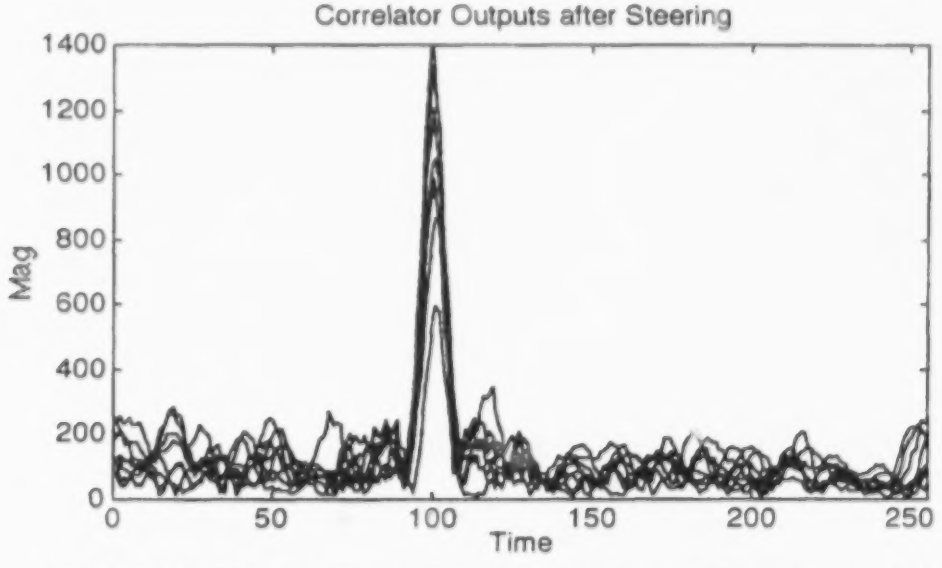

Fig. 3.4(a) As Fig. 3.1(b) but with t_1=101. Note no cancellation of signal near t_0=100

P516763.PDF [Page: 41 of 57]

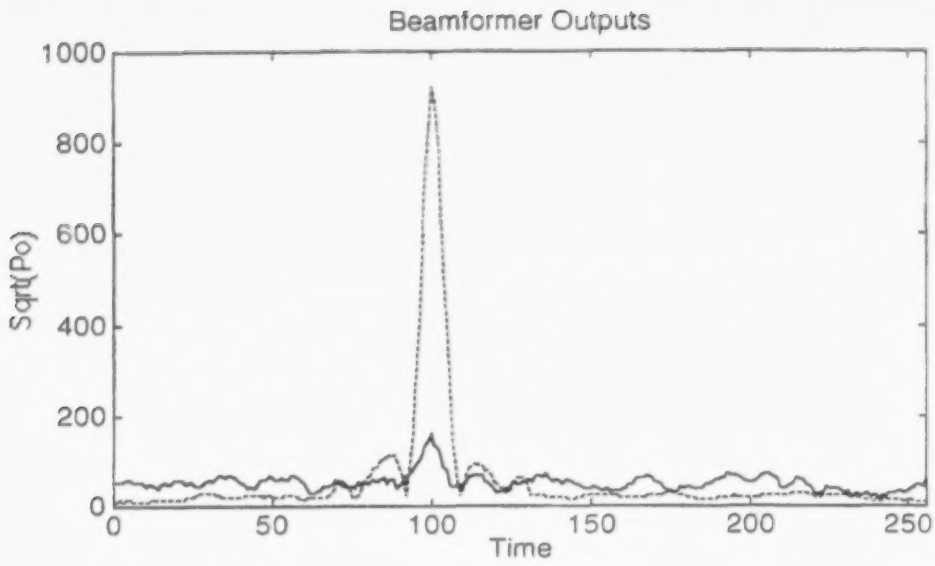

Fig. 3.4(b) Output from limacon beamformers (Averaged over eight realisations).
Note almost total cancellation of MVDR output near $t_0 = 100$.
Solid line = MVDR_LIM with 5 DOF, dashed lined = conventional beamformer (CB_LIM)

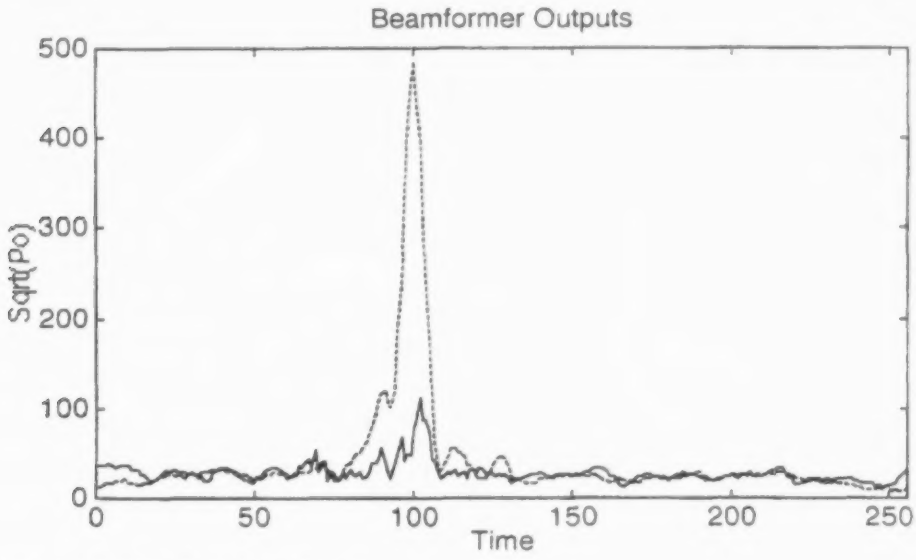

Fig. 3.4 (c) As Fig. 3.4(b) but $\theta_1 = 0$.
Note again cancellation of signal component by MVDR
Solid line = MVDR_LIM with 5 DOF, dashed lined = conventional beamformer (CB_LIM)

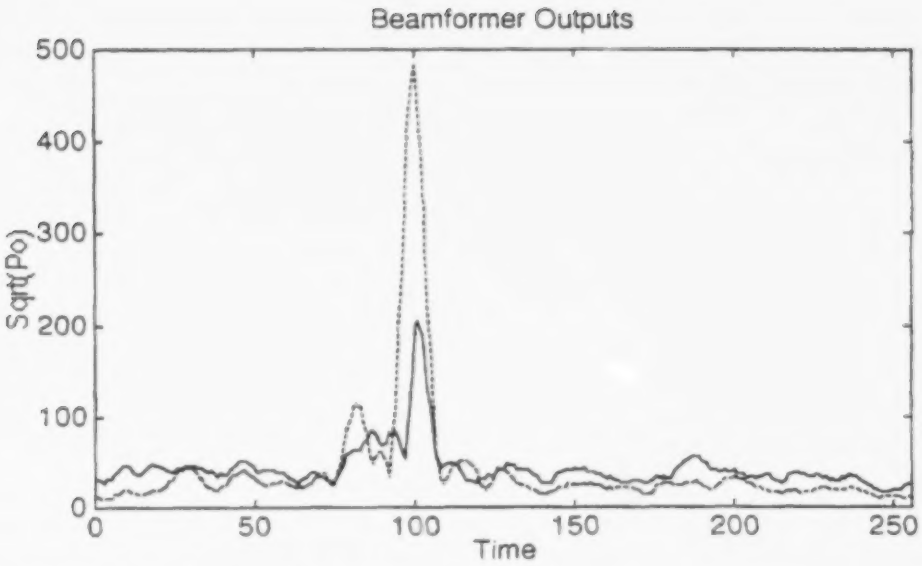

Fig. 3.4 (d) As Fig. 3.4(b) but $\theta_1 = 0.35\pi$.
Note again cancellation of signal component by MVDR beamformer.
Solid line = MVDR_LIM with 5 DOF, dashed lined = conventional beamformer (CB_LIM)

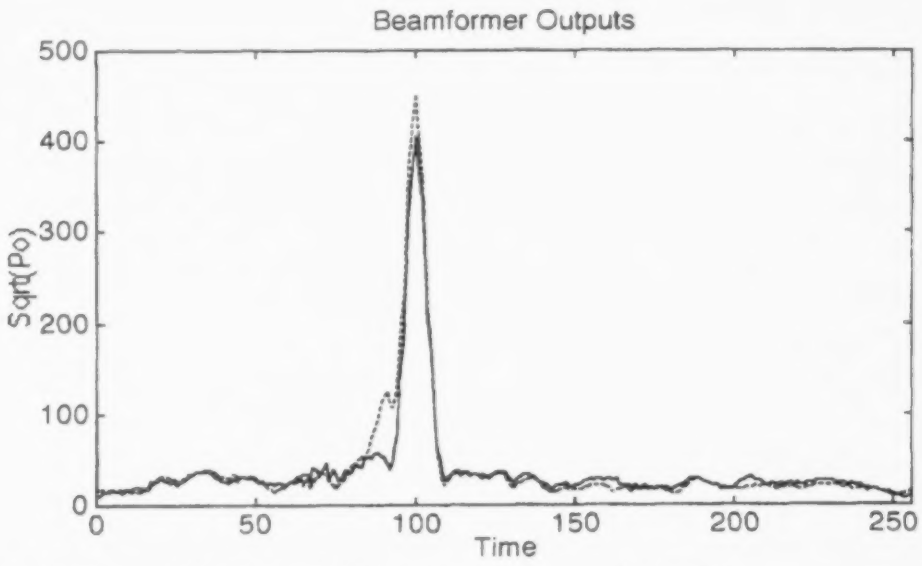

Fig. 3.5(a) As Fig. 3.3(c) ($\theta_1 = 0$) but with subarray averaging (N'=6).
Note signal component is no longer cancelled in MVDR output.
Solid line = MVDR_LIM with 5 DOF, dashed lined = conventional beamformer (CB_LIM)

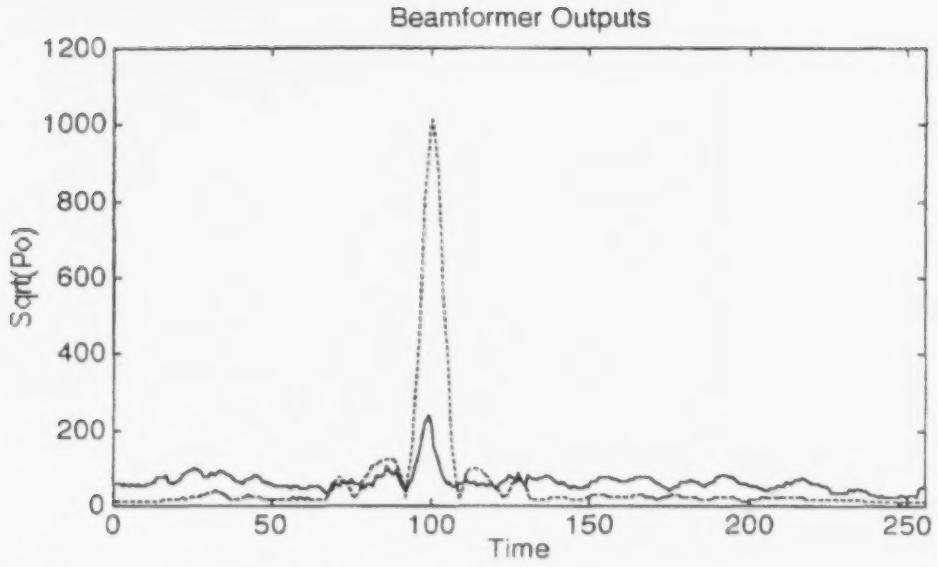

Fig.3.5(b) Close interference ($\theta_1 = 0.35\pi$).
Difficult to undo signal suppression even with subarray averaging (N'=6).
Solid line = MVDR_LIM with 5 DOF, dashed lined = conventional beamformer (CB_LIM)

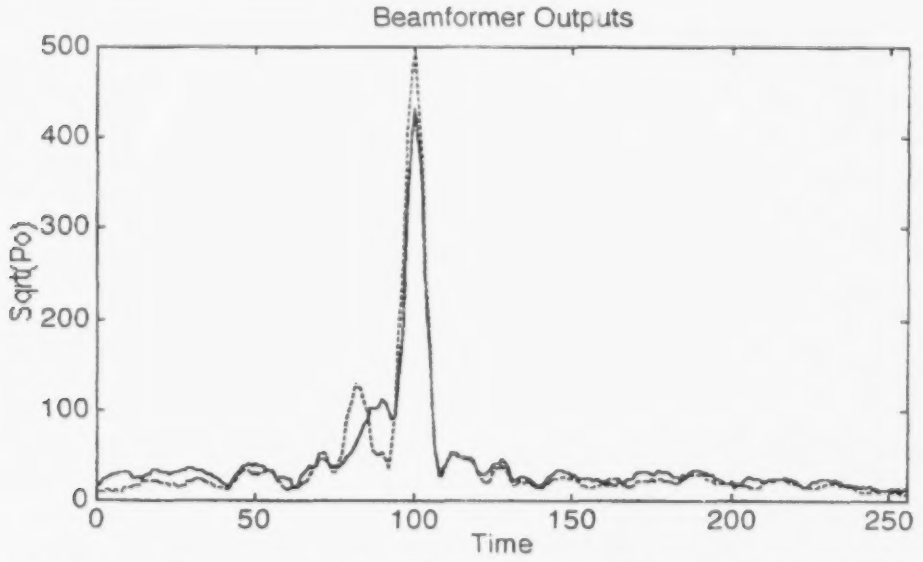

Fig. 3.5(c) Signal suppression effect undone with $\theta_1 = -0.35\pi$ and subarray averaging (N'=6).
Solid line = MVDR_LIM with 5 DOF, dashed lined = conventional beamformer (CB_LIM)

4. MVDR BEAMFORMING USING TWO PARALLEL ARRAYS.

4.1 Introduction

This section deals with MVDR beamforming by a pair of identical parallel arrays both lying in a horizontal plane. One array is a replica of the other but displaced in a horizontal direction. As in the previous section, we are interested in the ability of this twinned-array to deal with highly reverberant, 2-D fields where the primary signal is an FM chirp.

In the previous case, where we dealt with a single line array, nulling of interference from the "conjugate direction" was accomplished by setting the limacon parameters. In the twinned-array case, the sensor elements are assumed to be omni-directional and "conjugate nulling" may be performed either by adaptive means or by building the appropriate null into the quiescent beam pattern. In the former case the null is only created if necessary, that is, if there is an interferer at the conjugate angle but in the latter case the null always exists in that direction. In the former situation, adaptive degrees of freedom are not wasted. However, where it is required, the adaptive null is often not as deep as that produced by the quiescent strategy.

We shall also demonstrate that for the simple twinned-array approach to be effective, there is maximum allowable displacement between them which is related to the reciprocal of the chirp bandwidth multiplied by the acoustic speed of propagation.

4.2 Some numerical examples

We start by using a system where there is no effort to build a null into the quiescent beampattern of the twinned-array MVDR beamformer (2L_MVDR). The processing streams for each sensor are similar to that of the previous section where the arrays are pre-steered in the desired look direction and each sensor output is passed through a matched filter. Further, by using frequency domain methods, the outputs of the second array are time advanced/delayed to account for the propagation time differential, for a signal from the look direction, as measured between two corresponding sensors, one at the centre of each array, say. Thus for N sensors in each uniform line array, the desired-signal responses from the 2N matched filters are all time-aligned. However, this

is not true for the interference signal (if any) emanating from the conjugate direction where the time differential is actually doubled as a result of the processing.

Fig. 4.1 shows the results of an 2N=16 element 2L_MVDR beamformer where the array separation is half the inter-sensor separation of d=0.75m. The environment is similar to that described in the previous section. There is a signal arriving from azimuth angle of 0.45π (relative to broadside) at time 100 with a strength of 30 units. There are two interferers. One arrives from angle 0.35π at time 150 with an amplitude of 30 units; the other arrives from the conjugate angle (0.55π) at time 210 also with amplitude 30. The 2L_MVDR beamformer has five degrees of freedom (DOF=5) and the background reverberant noise level is about 5.5 units. Fig. 4.1 shows the results averaged over 32 realizations. The 2L_MVDR beamformer output is shown as the solid line, the output from the basic CB beamformer formed from one of the arrays is shown dotted. We see that the 2L_MVDR beamformer largely nulls out the conjugate interferer near time 210, and to a lesser extent, the close-in interferer (DOA = 0.35π) at time 150. We also note that the background level is raised in 2L_MVDR case (for instance, see around time 50) as a consequence of its having to deal with the spatially close interferer.

We now repeat the experiment but in this case a null at the conjugate angle is deliberately built into the MVDR beamformer's quiescent response. This beamformer is designated for convenience as 2L_MVDR_QN. If we let the 2L_MVDR_QN quiescent weight vector be written as the 2N x 1 vector, $\mathbf{w}_o$, then $\mathbf{w}_o$ is the minimum-norm solution to the under-determined matrix equation

$$\begin{bmatrix} \bar{1} & \bar{1} \\ \bar{1} & e^{j\gamma}\bar{1} \end{bmatrix} \mathbf{w}_o = \begin{bmatrix} 1 \\ 0 \end{bmatrix} \tag{4.1}$$

where $\bar{1}$ is a 1 x N vector of ones and γ is $4\pi f_o \tau$ where f_o is the centre frequency of the chirp and τ is the signal propagation delay measured between corresponding sensors in the two sub-arrays. It is understood that the upper N entries in $\mathbf{w}_o$ represent the weights for one of the line-arrays. The lower entries are the weights for the other array. The overall MVDR weight vector is written as (see equation (2.2a))

$$\mathbf{w} = \mathbf{w}_o - \mathbf{C}^H(\mathbf{C}\mathbf{R}\mathbf{C}^H)^{-1}\mathbf{C}\mathbf{R}\mathbf{w}_o \tag{4.2}$$

where the DOF x 2N blocking matrix $\mathbf{C}$ now has its rows orthogonal to each of the two rows of the constraint matrix (the matrix to the left of $\mathbf{w}_o$ in 4.1).

P516763.PDF [Page: 46 of 57]

In Fig. 4.2 we have the results equivalent to Fig. 4.1 but where the 2L_MVDR_QN beamformer has a null built in to the quiescent response. In comparison to Fig. 4.1, it seems that the interferences are somewhat more attenuated. However, even at the conjugate angle the cancellation is not perfect as the 2N-weight (i.e "single-tap") 2L_MVDR_QN beamformer of (4.1), (4.2) is essentially a narrowband approximation to the more appropriate wideband version. However, a true wideband MVDR beamformer would have to be of the multi-tap delay-line type with a concomitant increase in complexity.

If the desired signal at time 100 emanates from broadside (0π), we get the results of Fig. 4.3. Here we see that the interference effect near time 150 is reduced relative to the previous two figures (for both beamformers) and also that the 2L_MVDR_QN beamformer's background noise level is significantly lower as it no longer has to wrestle with a difficult "angularly close" interferer.

If we now double the spacing between the arrays so that it equals the inter-element spacing (0.75m) and re-run the previous experiment we get the results of Fig. 4.4. Of note in this case is the significant and undesirable increase in response to the conjugate interferer near time 210. This is entirely due to the deficiency in our single-tap quasi-narrowband model which cannot deal with the significant temporal separation in each sub-array's matched filter responses to the conjugate arrival. Note that time-alignment of the signal response must mean non-alignment of the interference response. If there is significant temporal separation then the (single-tap) beamformer finds it difficult to perform meaningful interference cancellation. In our particularly simple case, the signal angle is 0π, the conjugate angle is π and the propagation speed is 1500m/s, so the conjugate response separation will be about 2*0.75/1500 = 1ms. As the chirp bandwidth is 400Hz, the matched filter's sinc-type response is roughly of width 1/400 = 2.5ms so the separation is a significant fraction of the sinc's width, hence the cancellation difficulties. In essence, reasonable cancellation is only possible in a highly localized temporal region near time 210. If the inter-array spacing is increased further, we end up with two temporally distinct sinc-type responses for the conjugate signal with negligible cancellation. The temporal misalignment for the conjugate arrival is twice that of the propagation delay for the signal as measured between corresponding sensors, one in each sub-array. Thus is it worst for look-directions near broadside.

4.3 Summary

It has been demonstrated that the 2L_MVDR beamformer based on a twinned-array concept has useful interference cancellation properties in a highly reverberant field. Two issues are germane. The first involves the question of whether a null should be built into the quiescent beam pattern in the conjugate angle direction. If it is, then there are fewer adaptive degrees of freedom available for nulling other interferers and thus, if no interference actually exists near the conjugate angle, the beamformer's adaptive capabilities are being unnecessarily wasted. On the other hand, utilizing a quiescent null should guarantee better cancellation of any interference in the conjugate direction.

The second issue relates to the fact that our "single-tap" MVDR beamformer, (number of adaptive weights equal to the number of sensors) with no quiescent nulling of at the conjugate angle, can only perform cancellation of the conjugate interference if the inter-array spacing is not too large. Specifically, if the inter-array spacing is D, then we must have $D << c/(2\ BW)$ where c is the acoustic propagation speed and BW is the bandwidth of the chirp. From our experiments, it would seem that the maximum value of D is about $c/(10\ BW)$.

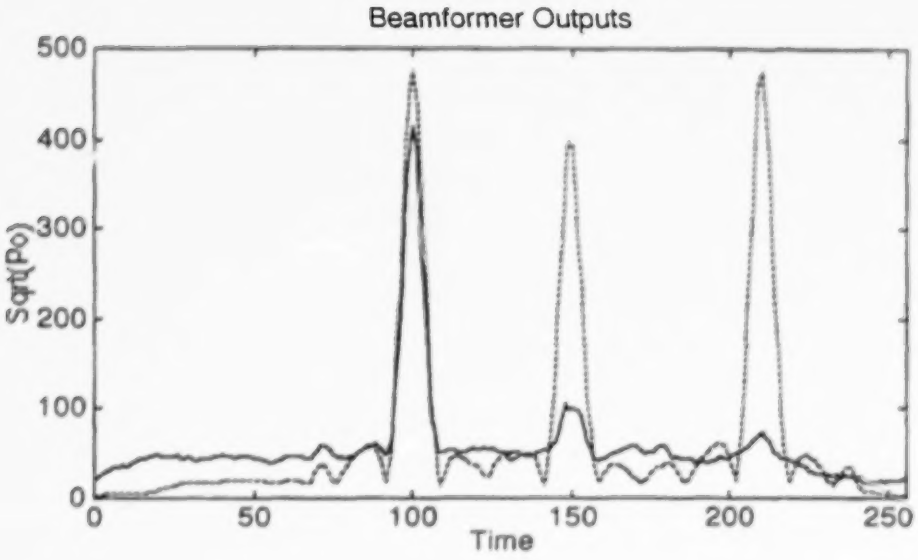

Fig. 4.1 Typical output time-series from beamformers. A_0 =30, θ_0= 0.45π, t_0 = 100; A_1 =30, θ_1= 0.35π, t_1 = 150; A_2 =30, θ_2= 0.55π, t_2= 210. Average over 32 realizations. Twinned-array 2L_MVDR (no quiescent null) _____ , CB ..... .

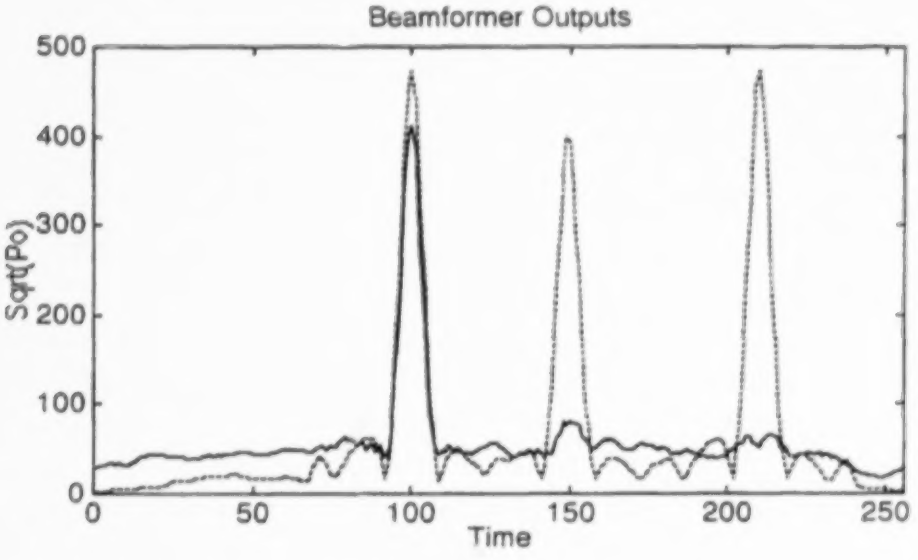

Fig. 4.2 As Fig 4.1 but with quiescent null in MVDR at conjugate angle (0.55π). Twinned-array 2L_MVDR_QN (with quiescent null) _____ , CB ..... .

P516763.PDF [Page: 49 of 57]

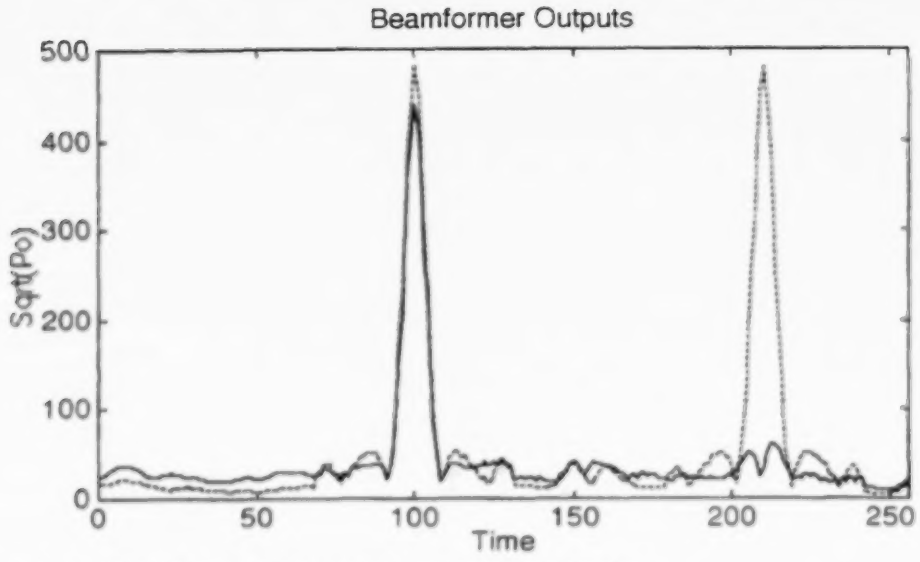

Fig. 4.3. As Fig. 4.2 but with desired signal at broadside (0π).
Twinned-array 2L_MVDR_QN (with quiescent null) _____ , CB ..... .

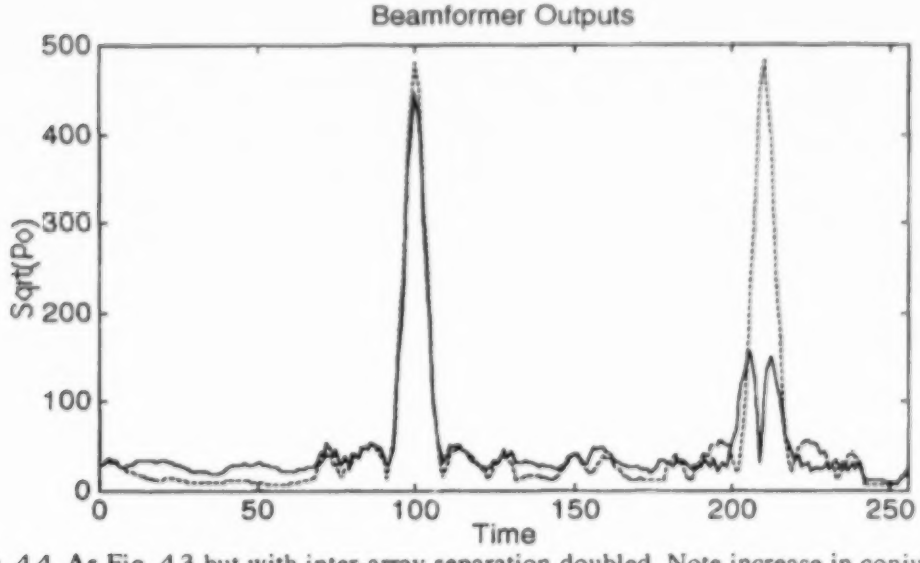

Fig. 4.4. As Fig. 4.3 but with inter-array separation doubled. Note increase in conjugate interference response near time 210.
Twinned-array 2L_MVDR_QN (with quiescent null) _____ , CB ..... .

5. SOME ELEMENTARY DETECTION STATISTICS

5.1 Power measurements

In order to evaluate the detection performance of each of the beamformer introduced earlier, one of the previous 2-D scenarios was rerun. In particular, we have a 32-point chirp signal with a 400Hz sweep of amplitude $A_0 = 10$, at angle $\theta_0 = 0.45\pi$ with arrival time 100; the conjugate arrival has amplitude 10 at sample time 210; and there is a interferer with amplitude 10 at angle 0.35π at time 150. The reverberations are each of unity amplitude and there are approximately 32 overlapping reverberation chirps with random phase angles at any time. The power output from the 8-element array system (16 in the case of the twinned array) steered in the signal direction at time 100 (where the output signal power is maximized) was averaged for each beamformer over 75 different realizations and designated as P_{100}. The experiment was repeated with the signal absent so essentially only noise is present at time 100. In the latter experiment the standard deviation of the 75 power estimates was also recorded. The results are summarized below.

Beamformer	P_{100} ($A_0 = 10$)	P_{100} ($A_0 = 0$)	std(P_{100} ($A_0 = 0$))
CB	2.53 E 4	224	242
MVDR	1.92 E 4	311	301
CB + LIM	2.51 E 4	469	479
MVDR + LIM	2.01 E 4	444	449
MVDR_2L	2.03 E 4	391	435
MVDR_2L + QN	1.99 E 4	594	629

Table 5.1. Output powers measured at time sample 100, with and without signal present.

5.2 SNR Analysis

The reverberation variance is approximately 32 units, while the signal power (A_0^2) at the sensor is about 100 units. Therefore the input SNR is $SNR_{in} = 3.1$ (or 5.0dB). We know that there will be a gain against the reverberation background given by the time-bandwidth product of the chirp which here is approximately ($32*2500^{-1}$ sec) x 400 Hz = 5.1. With an 8 element array, the CB would offer an array gain approaching 8, and thus the overall output SNR, CB_SNR_{out}, is expected to be about 3.1 x 5.1 x 8 = 126 (or 21.0dB). Using the data in Table 5.1 and noting

$$SNR_{out} = [\, P_{100}(A_0=10) - P_{100}(A_0=0) \,] \;/\; P_{100}(A_0=0) \qquad (5.1)$$

then this yields for the CB beamformer CB_SNR_{out} = 112 (20.5dB) which is close to the anticipated value of 126 (21.0dB).

For the basic MVDR beamformer we obtain $MVDR_SNR_{out}$ = 61 (17.9dB) . This is lower than the CB figure as output background noise level is higher (as a result of attempting to null the interference) together with a loss of signal power. The loss of signal power (about -1dB) is puzzling but is consistent across all the MVDR-based beamformers. The MVDR beamformer offers no attenuation against the conjugate arrival.

With the limacon-based line-array, which suppresses the conjugate arrival, the corresponding output SNR's are $CB_LIM_SNR_{out}$ = 53 (17.2dB) for the CB method and $MVDR_LIM_SNR_{out}$ = 44 (16.5dB) for the MVDR method. The background noise level is increased due to the limacon action, hence reducing the output SNR. In the CB method, there is actual amplification of the interference component at 0.35π., again due to the limacon action. This is not refected in the output SNR data.

Finally, the 2-line MVDR method (separation of d/2), excluding and including quiescent nulling of the conjugate signal, yields $2L_MVDR_SNR_{out}$ = 51 (17.1dB) and $2L_QN_MVDR_SNR_{out}$ = 33 (15.1dB), respectively. The latter figure represents the lowest output SNR of all the beamformers tested.

Comment: The above figures must be interpreted with extreme caution. For instance, the best SNR_{out} is given by the conventional CB. However, it offers no attenuation against the conjugate arrival, and negligible attenuation of the other interferer. Thus a complete picture is only given by a proper cost-benefit analysis which is very difficult to perform over a meaningful range of field scenarios. It has not been attepted here. In general, though, it seems that *a priori* ("quiescent") nulling in the conjugate arrival direction does lower the output SNR.

5.3 Deflection Factor Calculations

A simple measure used in elementary detectability studies is that of the deflection factor, δ, defined in our case as

$$\delta = [\, P_{100}(A_0=10) - P_{100}(A_0=0) \,] \;/\; \mathrm{std}(P_{100}(A_0=0)) \qquad (5.2)$$

It is the amount by which the mean signal power exceeds the mean background level, expressed in terms of the variability of the background distribution. It will be observed that equation (5.2) is identical to equation (5.1) with the denominator changed from $P_{100}(A_0=0)$ to $\mathrm{std}(P_{100}(A_0=0))$. However, a glance at Table 5.1 also reveals that $P_{100}(A_0=0)) \sim \mathrm{std}(P_{100}(A_0=0)$ so that the output SNR and the deflection factor are similar here. This is consistent with the familiar assumption that the background noise distribution in Gaussian based beamformer simulations, as used in this report, will follow a χ^2 distribution with two degrees of freedom, which in turn implies $P_{100}(A_0=0)) = \mathrm{std}(P_{100}(A_0=0)$.

5.4 Summary

An overall summary of output SNR and deflection factors is given in Table 2 below:

Beamformer	SNR_{out} (dB)	Deflection Factor (dB)
CB	20.5	20.2
MVDR	17.9	18.0
CB + LIM	17.2	17.1
MVDR + LIM	16.5	16.5
MVDR_2L	17.1	16.6
MVDR_2L + QN	15.1	14.8

Table 2 Summary of output SNR's and deflection factors

Again it should be cautioned that Table 5.2 says nothing about the effectiveness of each beamformer in suppressing (or not) the interference contributions.

6. CONCLUSION

This report has featured a numerical investigation into the performance of various MVDR-based adaptive beamformers operating in a wideband, highly-reverberant environment. A novel feature of this work is the application of MVDR techniques to a line array of limacon sensors, such limacons themselves having the ability to be "tuned" to eliminate the "conjugate arrival" problem. Though time constraints preclude the work from being exclusive, sufficient experiments were performed to allow the following observations to be made:

(1) The CB_LIM beamformer, while providing conjugate signal suppression, offers no attenuation against other interferers, some of which may well be amplified by the limacon action. This problem is exacerbated if the desired signal (or beam) angle is near endfire in which case interferences emanating from the broadside vicinity may be extensively amplified.

(2) The MVDR_LIM beamformer does offer complete conjugate signal suppression together with an ability to adaptively attenuate planewave interferences, both wideband and tonal. However, it is shown to be sensitive to strong multipath interferences whose arrival times are close to that of the desired signal. In such circumstances severe cancellation of the desired signal may occur even if the multipath arrival is angularly remote from the steering direction. It is further demonstrated that this effect can be reduced by using sub-array averaging as is routinely recommended in narrowband MVDR processing in multipath scenarios.

(3) The twinned-array beamformer (2L_MVDR) offers roughly similar performance to the MVDR_LIM. However, the conjugate arrival suppression is not as complete; the method is sensitive to the spacing between the arrays, which cannot exceed some maximum value; and the processing is more complex as there are double the number of adaptive weights to be computed. An advantage of the twinned-array method is that the conjugate arrival problem can be dealt with either adaptively, in which case a null is only built into the beampattern if necessary, thus freeing up degrees of freedom for nulling other interferers, or it may be

built into the quiescent MVDR weights, in which case a deep null always exists in the conjugate direction at the expense of reducing the adaptive number of degrees of freedom available for use elsewhere.

(5) In the simulation experiments performed here, there was no obvious discernible benefit in using the adaptive (MVDR) techniques in terms of performance in evolving reverberation backgrounds. This is interpreted as being a consequence of the relatively weak impact of the angularly diffuse regions of the background noise passing through the sidelobe structures of the different beamformers. However, MVDR methods are, as might be expected, advantageous if the noise is highly directive and within (or near) the main beam of the CB beamformer.

(6) All of the MVDR methods are amenable to implementation in so-called "partially adaptive" forms, thus somewhat reducing the computational burden.

P516763.PDF [Page: 55 of 57]

UNCLASSIFIED
SECURITY CLASSIFICATION OF FORM
(highest classification of Title, Abstract, Keywords)

DOCUMENT CONTROL DATA

(Security classification of title, body of abstract and indexing annotation must be entered when the overall document is classified)

1 ORIGINATOR (the name and address of the organization preparing the document. Organizations for whom the document was prepared, e g Establishment sponsoring a contractor's report, or tasking agency, are entered in section 8)

Dr. David N. Swingler, Division of Engineering
Saint Mary's University, Halifax, Nova Scotia B3H 3C3

2 SECURITY CLASSIFICATION (overall security classification of the document including special warning terms if applicable)

UNCLASSIFIED

3 TITLE (the complete document title as indicated on the title page. Its classification should be indicated by the appropriate abbreviation (S,C,R or U) in parentheses after the title)

Adaptive Array Processing in a Wideband Reverberant Environment

4 AUTHORS (Last name, first name, middle initial If military, show rank, e g Doe, Maj John E)

Dr. David N. Swingler

5 DATE OF PUBLICATION (month and year of publication of document)

October 2001

6a NO OF PAGES (total containing information Include Annexes, Appendices, etc)

41 (approx.)

6b NO OF REFS (total cited in document)

None

7 DESCRIPTIVE NOTES (the category of the document, e g technical report, technical note or memorandum. If appropriate, enter the type of report, e g interim, progress, summary, annual or final Give the inclusive dates when a specific reporting period is covered)

CONTRACTOR REPORT

8 SPONSORING ACTIVITY (the name of the department project office or laboratory sponsoring the research and development Include address)

Defence Research Establishment Atlantic
PO Box 1012
Dartmouth, NS, Canada B2Y 3Z7

9a PROJECT OR GRANT NO (if appropriate, the applicable research and development project or grant number under which the document was written Please specify whether project or grant)

Project 1CC11

9b CONTRACT NO (if appropriate, the applicable number under which the document was written)

W7707-5-3340/01-HAL

10a ORIGINATOR'S DOCUMENT NUMBER (the official document number by which the document is identified by the originating activity. This number must be unique to this document)

10b OTHER DOCUMENT NOs (Any other numbers which may be assigned this document either by the originator or by the sponsor)

DREA CR 2001-120

11 DOCUMENT AVAILABILITY (any limitations on further dissemination of the document, other than those imposed by security classification)

(X) Unlimited distribution
( ) Defence departments and defence contractors; further distribution only as approved
( ) Defence departments and Canadian defence contractors; further distribution only as approved
( ) Government departments and agencies; further distribution only as approved
( ) Defence departments; further distribution only as approved
( ) Other (please specify):

12 DOCUMENT ANNOUNCEMENT (any limitation to the bibliographic announcement of this document This will normally correspond to the Document Availability (11) However, where further distribution (beyond the audience specified in (11) is possible, a wider announcement audience may be selected)

UNCLASSIFIED

P516763.PDF [Page: 56 of 57]

13. ABSTRACT (a brief and factual summary of the document. It may also appear elsewhere in the body of the document itself. It is highly desirable that the abstract of classified documents be unclassified. Each paragraph of the abstract shall begin with an indication of the security classification of the information in the paragraph (unless the document itself is unclassified) represented as (S), (C), (R), or (U). It is not necessary to include here abstracts in both official languages unless the text is bilingual)

This contractor's report contains a detailed account of numerical simulations designed to measure the performance of various beamforming methods in highly reverberant wideband environments. The Minimum-Variance Distortionless-Response (MVDR) method is used in conjunction with a horizontal array of limacon sensors and a horizontal parallel array of omnidirectional sensors. The benefits and drawbacks of both configurations are weighed and discussed. Additionally, mathematical models for all scenarios discussed in this report are examined.

14. KEYWORDS, DESCRIPTORS or IDENTIFIERS (technically meaningful terms or short phrases that characterize a document and could be helpful in cataloguing the document. They should be selected so that no security classification is required. Identifiers, such as equipment model designation, trade name, military project code name, geographic location may also be included. If possible keywords should be selected from a published thesaurus, e.g. Thesaurus of Engineering and Scientific Terms (TEST) and that thesaurus identified. If it not possible to select indexing terms which are Unclassified, the classification of each should be indicated as with the title)

Active sonar
Adaptive beamforming
Line array
Minimum variance
Wideband FM
Reverberation noise

P516763.PDF [Page: 57 of 57]

Defence R&D Canada
is the national authority for providing
Science and Technology (S&T) leadership
in the advancement and maintenance
of Canada's defence capabilities.

R et D pour la défense Canada
est responsable, au niveau national, pour
les sciences et la technologie (S et T)
au service de l'avancement et du maintien des
capacités de défense du Canada.

#5167 63
CAOOC11

DEFENCE R&D DÉFENSE

www.drdc-rddc.dnd.ca